Nano Research

Open Access

Review Article

# Myocardial repair strategy based on force-electrical regulation and bionic platform

Mengke Zhu[1,2,§], Jie Mei[2,§], Jing Yuan[5,§], Yan Ren[1], Xin Huang[2,3,4], Zibo Chen[6], Minxuan Jia[2,3,4], Chubing Lin[2,3,4], Yueguang Xue[2,3,4], Yi Liu[2], Cuiqing Liu[1] ✉, Ying Liu[2] ✉, and Shanshan Xu[6] ✉

[1] *School of Public Health, Zhejiang Chinese Medical University, Hangzhou 310053, China*
[2] *CAS Key Laboratory for Biomedical Effects of Nanomaterials and Nanosafety & CAS Center for Excellence in Nanoscience, National Center for Nanoscience and Technology of China, Beijing 100190, China*
[3] *GBA National Institute for Nanotechnology Innovation, Guangzhou 510535, China*
[4] *School of Biomedical Science and Engineering, South China University of Technology, Guangzhou 510006, China*
[5] *Department of Pathology, the First Medical Center of Chinese PLA General Hospital, Beijing 100853, China*
[6] *Institute for Advanced Study, Shenzhen University, Shenzhen 518060, China*
[§] *Mengke Zhu, Jie Mei, and Jing Yuan contributed equally to this work.*

**Cite this article:** *Nano Research*, **2026**, *19*, 94908608. https://doi.org/10.26599/NR.2026.94908608

**ABSTRACT:** Myocardial infarction causes structural damage that impairs both the mechanical and electrophysiological functions of the heart. Modulating the mechanical and electrical properties of biomaterials represents a promising strategy for myocardial repair. This review systematically outlines the mechanisms and design principles of such regulation through three integrated approaches: mechanical modulation, electrical modulation, and mechano-electrical coordination. Mechanically, tuning stiffness, elasticity, and anisotropy enhances cellular alignment, tissue integration, and structural support. Electrically, regulating conductivity and anisotropy facilitates synchronous signal propagation and functional restoration. The coordinated strategy enables synergistic optimization of mechanical and electrical properties, thereby improving repair outcomes. Furthermore, biomimetic *in vitro* models, including cardiac organoids and heart-on-a-chip systems, provide physiologically relevant platforms for evaluating material performance. This review provides foundational insights and design principles for advancing myocardial repair via mechano-electrical biomaterial engineering.

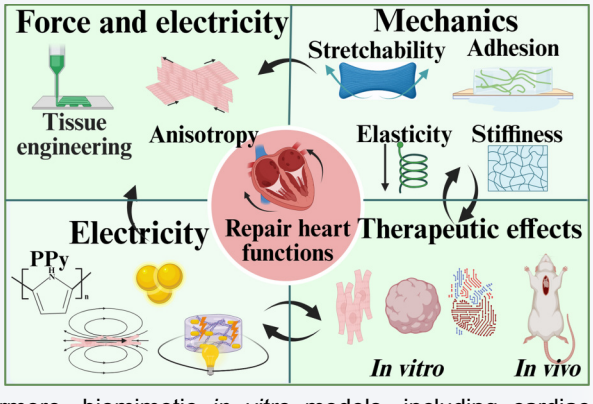


**KEYWORDS:** myocardial repair, biomaterials, mechanical modulation, force-electrical regulation, bionic models

## 1 Introduction

Myocardial infarction (MI) is clinically defined as an acute myocardial injury evidenced by elevated cardiac biomarkers, particularly troponin, accompanied by clinical manifestations of acute myocardial ischemia. Based on electrocardiographic characteristics, MI is classified into two main types: ST-segment elevation MI (STEMI) and non-ST-segment elevation MI (NSTEMI) [1]. In 2019, cardiovascular diseases accounted for 18.6 million deaths worldwide, with ischemic heart disease (9.1 million) and stroke (6.6 million) comprising approximately 85% of all cardiovascular-related mortality [2]. According to the Global Burden of Disease Study (2019), the prevalence of cardiovascular diseases is projected to increase by 90% between 2025 and 2050, reaching an estimated 35.6 million deaths globally, among which ischemic heart disease will remain the leading cause, responsible for approximately 20 million deaths [3]. The primary pathophysiological cause of MI is the rupture or erosion of atherosclerotic plaques within the coronary arteries, leading to thrombus formation, coronary occlusion, and myocardial ischemia [4]. Multiple risk factors contribute to its onset, including dyslipidemia, smoking, obesity, gender, unhealthy lifestyle habits, and genetic predispositions such as coagulation disorders or gene mutations [2, 5]. Current therapeutic approaches include oxygen

**Received:** December 23, 2025; **Revised:** February 24, 2026
**Accepted:** February 27, 2026

✉Address correspondence to Cuiqing Liu, liucuiqing@zcmu.edu.cn; Ying Liu, liuy@nanoctr.cn; Shanshan Xu, xuss@szu.edu.cn

therapy, pharmacological interventions (e.g., antiplatelet agents, β-blockers, angiotensin-converting enzyme inhibitor (ACEI)/angiotensin II receptor blockers (ARBs)), coronary angiography (CAG), percutaneous coronary intervention (PCI), coronary artery bypass grafting (CABG), and adjunctive rehabilitation therapies [4]. Although these treatments effectively restore perfusion in the acute phase and reduce early mortality, long-term outcomes remain suboptimal. A national Danish cohort reported a 5-year mortality of 12.5%, recurrent MI of 5.5%, and bleeding risk of 2.7% [6]. Moreover, the dangers of non-cardiovascular complications increased by 38.6% and 64.8% at 1 and 5 years post-MI, respectively [7]. Despite advances in acute management, current therapies fail to achieve proper myocardial regeneration, leaving patients vulnerable to progressive ventricular remodeling and cardiac dysfunction. Therefore, novel therapeutic strategies to promote myocardial regeneration are urgently needed.

Force-electrical synergistic biomaterials are functional materials that combine tunable mechanical properties with electrical signal conduction, enabling the simulation or regulation of the coupled mechanical and electrophysiological effects observed in biological tissues. These materials have demonstrated broad potential for repairing diverse tissues, including nerves [8], bones [9], skin [10], wounds [11], and hearts [12, 13]. The heart relies on the highly coordinated interplay of mechanical and electrical signals to regulate rhythmic myocardial contraction and maintain efficient blood pumping. Gap junctions and intercalated discs facilitate rapid electrical propagation and mechanical force transmission, ensuring synchronous myocardial contraction and relaxation [12]. Dynamic mechanical biomaterials with adjustable topography and stiffness have been shown to promote cardiomyocyte maturation and tissue formation [12]. Nanofiber-hydrogel composite scaffolds can mimic the heart's highly organized anisotropic structure, guiding orderly cell alignment and enhancing functional maturation [14]. Conductive materials further improve intercellular electrical signal transmission by accelerating the maturation of electrically responsive cells, increasing ionic conductivity, and reducing infarct tissue resistivity, thereby supporting the restoration of cardiac rhythm [13]. Several force-electrical synergistic materials have already been applied in cardiac repair. For example, mechanically-electrically coupled hydrogel patches (MEHPs) constructed via dynamic cross-linking combine adaptive viscoelasticity with electrical conductivity, enabling responsiveness to myocardial contraction-relaxation cycles while establishing electrical bridges within the infarcted region to restore synchronous electrophysiological function [15]. Moreover, emerging fabrication techniques such as 3D printing, electrospinning, and microfluidics, together with advanced organoids and organ-on-a-chip models, further facilitate the MI repair [16].

This article focuses on the research and application of force-electrical coupling materials for MI repair. Considering the heart's reliance on coordinated mechanical contraction and synchronous electrical signaling for proper function, the paper first reviews the mechanical and electrophysiological characteristics of cardiac tissue under both healthy and pathological conditions, followed by an analysis of the force-electrical microenvironment disruptions induced by MI. This paper systematically summarizes the design principles and functional properties of existing biomaterials, which encompass electrical conductivity, mechanical compatibility, and microenvironmental modulation. It also elaborates on their application strategies aimed at reconstructing electrical conduction networks, restoring mechanical support, and promoting tissue regeneration. Furthermore, the article highlights the significant role of emerging *in vitro* platforms, such as cardiac organoids and organ-on-a-chip systems, in evaluating material performance. Overall, this work aims to provide theoretical guidance and practical insights for the development of cardiac repair materials with enhanced biomimicry and therapeutic efficacy (Fig. 1).

## 2 Biophysical basis of force-electrical synergy in the myocardium

### 2.1 Coordinated mechanical and electrical function in the healthy heart

The heart is an intelligent pump composed of multiple cell types that function in coordination. Working cardiomyocytes and pacemaking/conduction cells are responsible for mechanical contraction and the generation and propagation of electrical signals, respectively, thereby jointly maintaining rhythmic pumping activity [17, 18]. From the perspectives of physics and biophysics, the heart is a highly integrated, tightly coupled force-electrical system in which mechanical forces and electrical stimuli interact dynamically and bidirectionally across multiple scales [19].

During each cardiac cycle, cardiomyocytes continuously experience variations in preload, afterload, and ventricular wall stress, which are perceived as active physical stimuli by myocardial tissue [20]. Mechanical signals are primarily sensed through mechanotransduction processes at the cell membrane and at the protein level. On the one hand, mechanical deformation directly affects the lipid bilayer of the cell membrane, altering its area, thickness, and surface charge distribution, thereby modulating the transmembrane electric field and membrane potential. On the other hand, mechanical stimulation induces conformational changes in force-sensitive proteins, converting mechanical signals into electrical and intracellular chemical signals, and consequently, regulating their electrical conductivity or signaling activity [19, 21]. Through these pathways, mechanical stimuli can directly influence membrane potential and action potential morphology, thereby generating mechano-electrical feedback (MEF). Studies have shown that when the myocardium is subjected to tensile or pressure loading, mechanically sensitive ion channels, such as non-specific cation channels (SACns), Piezo1, transient receptor potential canonical 6 (TRPC6), and ATP-sensitive $K^+$ (KATP) channels, are activated, resulting in alterations in action potential duration and repolarisation dynamics and ultimately affecting cardiac rhythm stability [20].

The pacing signal originating in the sinoatrial node (SAN) in the right atrium initiates electrical excitation of cardiomyocytes, forming an orderly wave of action potentials (APs). Through the excitation–contraction coupling (ECC) process, electrical signals are subsequently converted into mechanical contraction [22]. This process is not a unidirectional linear conduction pathway but rather a highly dynamic and bidirectional physicochemical interaction system. Action potential depolarisation activates voltage-gated L-type $Ca^{2+}$ channels (ICa-L), and the resulting small influx of $Ca^{2+}$-triggers a larger release of $Ca^{2+}$ from the sarcoplasmic reticulum via ryanodine receptors. The spatiotemporal integration of local $Ca^{2+}$ sparks generates global $Ca^{2+}$ transients, which ultimately drive myofilament sliding and induce myocardial contraction. This represents the core process by which electrical energy is converted

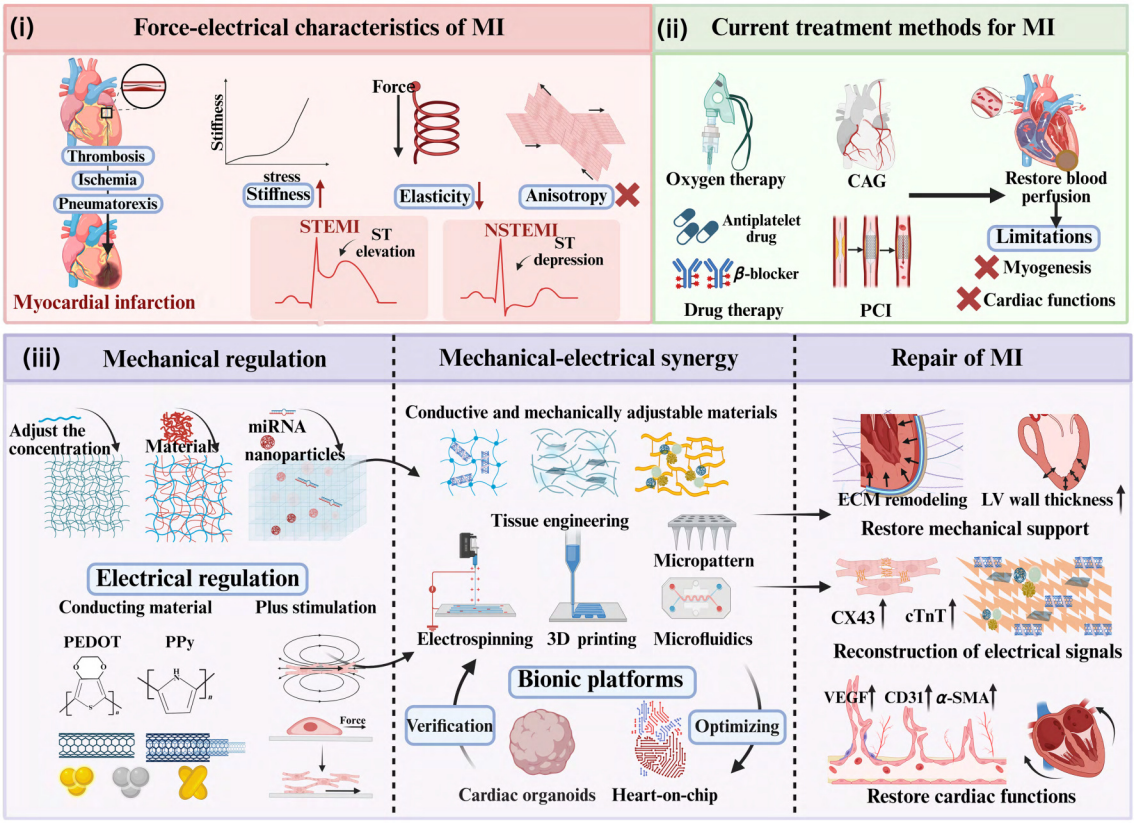


**Figure 1** Promising strategies for MI repair based on force-electrical regulation and bionic platform. (i) MI is primarily caused by thrombosis or coronary artery obstruction, resulting in ischemia and hypoxia of cardiomyocytes. Following infarction, the myocardium undergoes pronounced alterations in its force-electrical properties, including significant changes in mechanical characteristics such as stiffness, elasticity, and anisotropy. Concurrently, these pathological changes are reflected in electrocardiographic manifestations, and MI is clinically classified as ST-segment elevation MI (STEMI) or non-ST-segment elevation MI (NSTEMI). (ii) Although conventional therapeutic approaches, such as oxygen therapy, pharmacological treatment, coronary angiography, and percutaneous coronary intervention, can rapidly restore myocardial perfusion during the acute phase, they remain limited in promoting myocardial tissue regeneration and fail to achieve complete functional recovery of the heart. (iii) Following MI, the force-electrical characteristics of the myocardium undergo significant alterations, resulting in impaired cardiac function. Emerging strategies aim to restore cardiac performance by developing functional materials with tunable mechanical and electrical properties, in combination with tissue engineering approaches to reconstruct the heart's intrinsic anisotropic architecture. Meanwhile, bionic platforms such as cardiac organoids and heart-on-a-chip systems enable more physiologically relevant modeling of pathological conditions, as well as assessment and screening of material repair efficacy, thereby providing valuable insights for material optimization and facilitating clinical translation (figure was created with BioRender.com).

into chemical signals (calcium signaling), which, in turn, drive mechanical contraction [23, 24].

Calcium ion-mediated chemical signaling plays a central role in force-electrical synergy in cardiomyopathy, serving as an intermediary linking mechanical stimulation and electrical activity [25]. At the cellular scale, the amplitude, timing, and spatial heterogeneity of $Ca^{2+}$ transients not only determine contractile force magnitude but also participate in membrane repolarisation by modulating calcium-dependent currents, thereby shaping action potential kinetics and electrical stability in a reciprocal manner. Meanwhile, mechanical tension and changes in load can directly regulate the opening probability of calcium release channels and the activity of calcium reuptake pumps, enabling mechanical states to be encoded into calcium signals in real time and subsequently fed back into electrical activity [23]. At the tissue and subcellular scales, variations in sarcomere length and myocardial strain regulate myofilament sensitivity to $Ca^{2+}$, influence the function of calcium-handling proteins, and activate signaling pathways associated with length-dependent activation and load-induced positive inotropic responses, including the Frank-Starling mechanism and the Anrep effect [26]. Furthermore, the proposed voltage-sensitive release mechanism (VSRM) suggests that membrane potential can directly regulate intracellular $Ca^{2+}$ release, even under conditions of weak dependence on extracellular $Ca^{2+}$ influx, thereby providing additional biophysical regulatory pathways for myocardial contraction [27, 28].

The heart's characteristic force-electrical properties originate from the dynamic bidirectional coupling between electrophysiological activity and mechanical contraction. By integrating electrical propagation, calcium handling, and mechanical output across scales, this coupling sustains stable and efficient cardiac pumping. Disruption of this finely coordinated system, caused by structural remodeling, mechanical alterations, or conduction abnormalities, destabilizes force-electrical synergy and increases the risk of arrhythmia. Therefore, understanding the physical basis of cardiac force-electrical coupling is essential for both elucidating normal physiology and guiding reconstruction under pathological conditions.

### 2.2 Disruption of force-electrical synergy following myocardial infarction

After MI, necrotic myocardium is replaced by fibrotic scar tissue,

leading to a force-electrical imbalance characterized by abnormal electrical activity and impaired contractility. The infarcted region exhibits markedly altered mechanical properties compared with healthy myocardium, including increased stiffness, reduced contractile capacity, altered anisotropy, and disrupted extracellular matrix (ECM) composition, all of which compromise global mechanical conduction and cardiac coordination (Fig. 2) [29–31]. Experimental studies have demonstrated that the elastic modulus of remote rat myocardium increases from approximately 18 kPa in normal tissue to 55 kPa after MI, indicating a substantial increase in stiffness [32]. Computational modeling further reveals that the left ventricular ejection fraction (LVEF) decreases from 63% in healthy hearts to 56%, 51%, and 52% in ischemic, acute, and chronic MI models, respectively. Meanwhile, active contractility declines, whereas passive stiffness parameters can increase by up to 200-fold [33]. ECM remodeling plays a central role in this pathological process. MI induces extensive ECM degradation and fibrosis, disrupting cellular signal transduction, impairing cardiomyocyte function, and weakening cell-matrix interactions, ultimately compromising overall cardiac performance. Elevated expression of matrix metalloproteinases (MMP-2 and MMP-9) accelerates ECM degradation, resulting in ventricular wall thinning, and in severe cases, rupture [34]. ECM components undergo dynamic reconstruction throughout MI progression. In rat models, periostin expression increases approximately fivefold within the first week after MI. In the fourth week, type I collagen constitutes 57% of the total ECM compared with only 16% in normal myocardium [35, 36]. These compositional and structural alterations of the ECM contribute not only to tissue stiffening, serving as a temporary defense against rupture, but also to impaired diastolic compliance in the infarcted and adjacent regions.

MI patients typically exhibit characteristic electrocardiographic abnormalities, such as ST-segment depression and T-wave inversion, primarily resulting from disruptions in ionic mechanisms governing cardiac electrical activity (Fig. 2(ii)). During acute MI, the rapid sodium current (INa) in junctional cardiomyocytes is inhibited by approximately 42.5%. In comparison, both the rapid delayed rectifier potassium current (IKr) and the transient outward potassium current (Ito) are almost completely abolished (reduced by nearly 100%). Concurrently, the autophosphorylation level of $Ca^{2+}$/calmodulin-dependent protein kinase II (CaMKII) increases by about 50%, thereby delaying calcium release [33]. These ionic and signaling abnormalities collectively alter the morphology and conduction characteristics of the action potential, contributing to electrophysiological remodeling following MI. Due to the formation of fibrotic scar tissue, myocardial resistivity increases from a standard range of 200–300 to 400–500 Ω·cm, impeding action potential propagation [37]. Moreover, the expression and distribution of the gap junction protein connexin 43 (Cx43) are markedly altered, further slowing or blocking electrical conduction and predisposing to arrhythmias [38]. In ischemia-induced rat models, Cx43 undergoes significant dephosphorylation during electrotonic coupling, with non-phosphorylated isoforms abnormally accumulating at gap junctions and translocating from intercellular junctions to intracellular storage pools [39]. Collectively, these findings indicate that MI induces ion channel

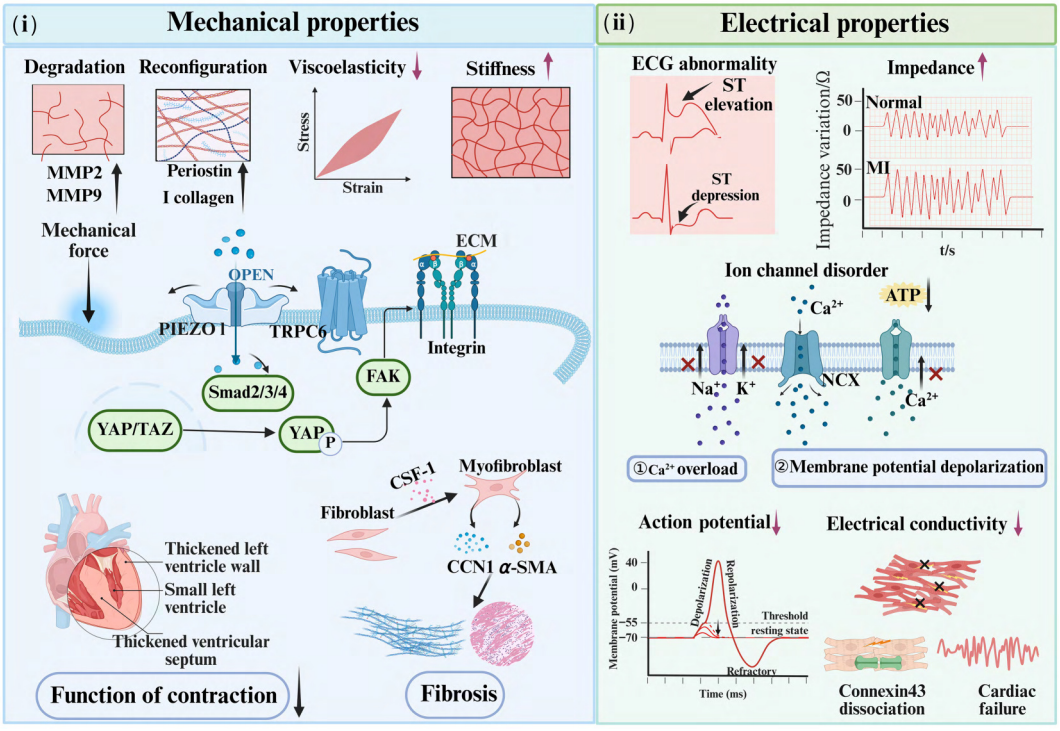


**Figure 2** Force-electrical imbalance after MI. (i) Mechanical changes: the activity of MMPs is markedly upregulated, resulting in ventricular wall thinning and ECM remodeling. Consequently, key mechanical properties, including tissue viscoelasticity, stiffness, adhesion, and anisotropy, are significantly altered. These mechanical cues are sensed by mechanosensitive ion channels and integrin-mediated receptors, triggering downstream signaling cascades that ultimately impair myocardial contractility and promote fibrotic remodeling. (ii) Electrical changes: MI is also characterized by typical electrocardiographic abnormalities, including ST-segment elevation and non-ST-segment elevation patterns, along with increased myocardial electrical impedance. These alterations arise from disrupted ionic homeostasis, which diminishes potential amplitude, impairs electrical conduction, and downregulates connexin Cx43 expression. Consequently, these electrophysiological disturbances can precipitate arrhythmia and, in severe cases, progress to heart failure (figure was created with BioRender.com).

dysfunction, increased tissue resistivity, and aberrant expression and redistribution of Cx43, thereby impairing the electrical conduction capacity of cardiomyocytes.

After MI, mechanical heterogeneity promotes ectopic excitation and abnormal electrical conduction. During cardiac contraction, cardiomyocytes in the ischemic border zone undergo abnormal elongation due to impaired contractile function, resulting in elevated mechanical tension that predisposes this region to ectopic electrical activity [19]. Computational models indicate that mechanically induced depolarization in ischemic myocardium can slow or block conduction by reducing local excitability under conditions of hyperkalemia [40]. Following MI, impaired $Ca^{2+}$ handling and sarcoplasmic reticulum (SR) dysfunction disrupt ECC. Although action potentials can still be generated in response to electrical stimulation, the $Ca^{2+}$-triggered contractile response fails to effectively translate into mechanical force, resulting in delayed relaxation and prolonged contraction [41]. In rat MI models, blockade of L-type $Ca^{2+}$ channels has been shown to reduce cardiomyocyte contractility by approximately 50% [42]. The resulting force-electrical imbalance further exacerbates disturbances in both electrophysiological and mechanical functions, predisposing to arrhythmias, progressive heart failure, and, in severe cases, sudden cardiac death.

## 3 Material strategies to enhance force-electrical synergy for myocardial repair

Under physiological conditions, myocardial tissue operates within a complex dual regulatory environment involving both mechanical tension and electrical signal conduction. Following MI, disruption of this electromechanical microenvironment results in disorganized cellular architecture, impaired signal transmission, and reduced cardiac contractile function [43, 44]. Therefore, restoring mechanical support and re-establishing electrophysiological connectivity in the infarcted region have become critical goals in cardiac repair strategies. In recent years, biomaterials with tunable mechanical properties and electrical activity have been continuously developed, evolving from single-function systems to multifunctional platforms capable of coordinated regulation of both cues. Such advancements provide new avenues for reconstructing myocardial function and enhancing post-infarction recovery [45–47]. To better understand this progression, the following sections first outline the historical evolution of mechanical and conductive materials for myocardial repair and then summarize current design strategies aimed at achieving precise electromechanical modulation.

### 3.1 Material strategies to enhance force-electrical synergy for myocardial repair

#### *3.1.1 Evolution of mechanical materials for myocardial repair*

The pathological progression following MI can be broadly divided into three distinct yet overlapping stages: the inflammatory stage, the repair and proliferation stage, and the maturation stage [48]. Throughout this process, the ECM undergoes pronounced mechanical remodeling. During the inflammatory phase, matrix metalloproteinases (MMPs) are rapidly activated and degrade major ECM components, leading to disruption of the native structural architecture and a marked reduction in local mechanical integrity [34]. In the subsequent repair and proliferation phase, activated fibroblasts differentiate into myofibroblasts and promote excessive collagen deposition. This process progressively increases ECM stiffness and ultimately contributes to pathological fibrosis with non-physiological mechanical properties [49]. At the maturation stage, the ECM mechanical environment gradually stabilizes. Activated myofibroblasts deploy-SMA stress fibres and transition toward a more quiescent stromal fibroblast phenotype. Their role shifts from active matrix remodeling to maintaining scar stability and sustaining ECM protein secretion [50]. The continuous mechanical transition of the ECM, from acute degradation to chronic stiffening, drives adverse ventricular remodeling and progressive functional decline [51]. Therefore, an effective myocardial repair strategy should not be limited to providing passive mechanical support. Instead, it should be designed to dynamically match or actively modulate the evolving mechanical properties of the ECM across different pathological stages, thereby intervening in the remodeling process and improving functional outcomes.

Based on insights into the dynamic mechanical changes of the cardiac ECM, the design paradigm of myocardial repair materials has gradually shifted from providing simple mechanical support to enabling precise mechanical regulation and structural biomimicry. From the 1990s to the early 21st century, myocardial repair strategies primarily employed natural biomaterials such as collagen, fibrin, and alginate [52, 53]. These materials served as cell carriers, or scaffolds, providing fundamental structural support for cardiomyocytes and constituting a cornerstone of early tissue-engineering approaches [54, 55]. Later, natural ECM-derived materials, including acellular heart matrices, were adopted to construct scaffolds with enhanced biological activity that better recapitulate the native ECM environment [56]. However, at this stage, material design primarily focused on structural filling and biocompatibility optimization. Precise control over mechanical properties remained challenging, and some naturally sourced materials carried potential immunogenicity risks, limiting their capacity to provide stage-specific mechanical support and thereby constraining long-term repair outcomes [57, 58]. To overcome the limited tunability of natural matrices, researchers gradually introduced synthetic hydrogel systems, such as gelatin methacryloyl (GelMA) and chitosan-based materials [59, 60]. As tissue engineering advances and myocardial mechanical anisotropy becomes increasingly appreciated, material design has transitioned toward anisotropic structural constructs. [61, 62]. This transition marked a critical shift from passive structural replacement toward controllable mechanical regulation. Moreover, achieving robust adhesion within the dynamic cardiac microenvironment remains a crucial barrier to clinical translation. The requirement for secure fixation under continuous myocardial motion has driven the development of adhesive and self-anchoring systems, including Janus hydrogel patches and GRAXe-based constructs, designed to enhance interfacial stability *in vivo* [63, 64].

Overall, myocardial repair materials have evolved from natural ECM scaffolds to tunable synthetic hydrogels and structurally engineered anisotropic constructs. The design paradigm has progressed from providing passive mechanical support to enabling multidimensional regulation of mechanical and functional properties. Current strategies focus on reconstructing the mechanical microenvironment by precisely tuning stiffness, anisotropy, and adhesive cues to better approximate physiological conditions. These optimizations enhance cardiomyocyte survival, promote angiogenesis, modulate immune responses, and improve

tissue integration, thereby supporting coordinated cardiac repair (Fig. 3(a)).

### 3.1.2 *Design strategies for matching cardiac mechanical properties*

After MI, the left ventricle frequently undergoes wall thinning and dilation, leading to adverse remodeling and progressive dysfunction [51]. To address these challenges, contemporary mechanical biomaterials are rationally constructed through modular design strategies, primarily involving (i) modulation of stiffness and elasticity, (ii) anisotropic structuring, and (iii) adhesion engineering.

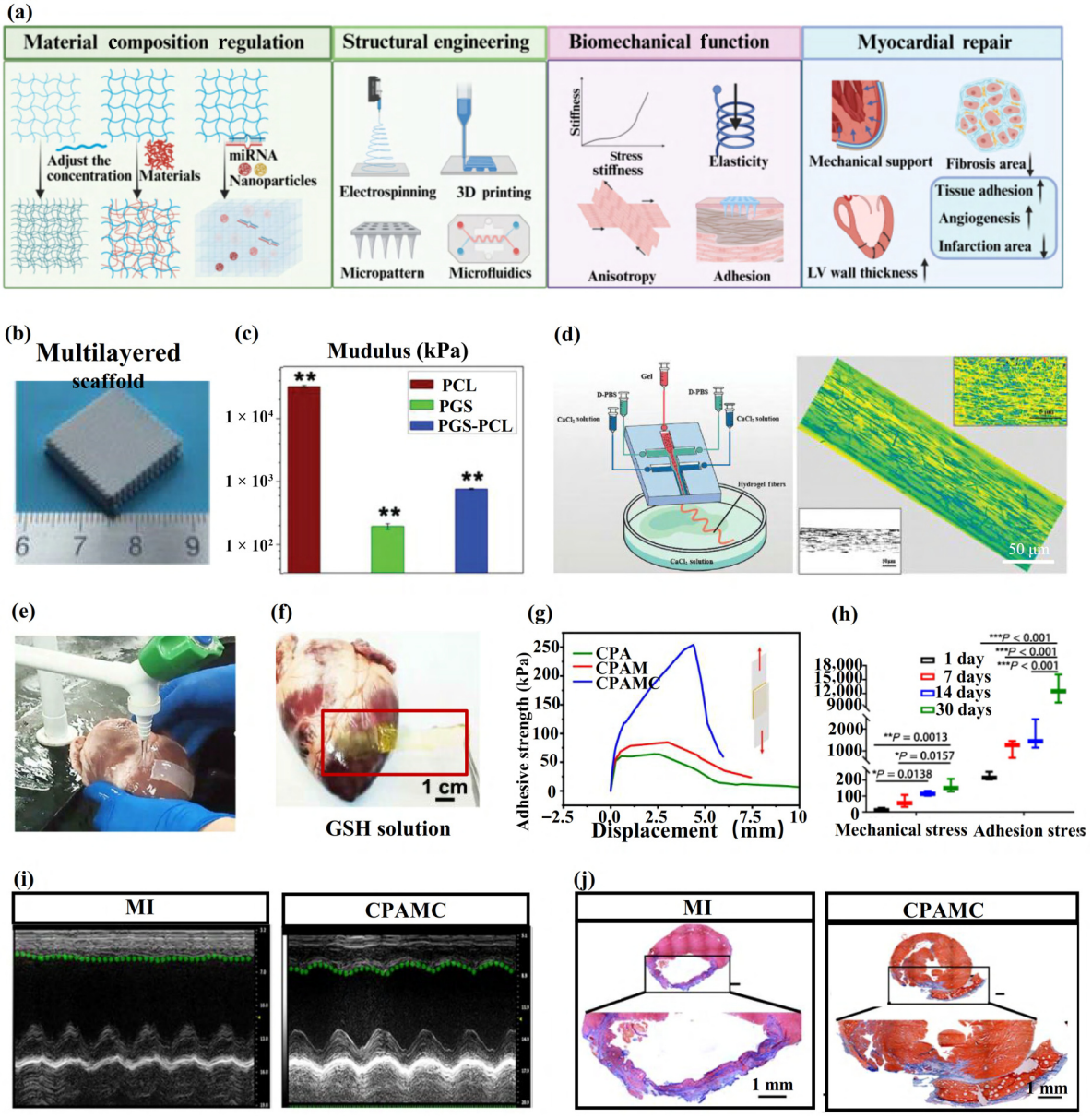


**Figure 3** Reconstruction of mechanical support for the heart through mechanical regulation. (a) By regulating material concentration, incorporating different components or functional additives, and integrating tissue engineering techniques such as electrospinning, 3D printing, and micropatterning, the mechanical properties of materials, including stiffness, elasticity, anisotropy, and adhesion, can be precisely tuned. These optimized materials provide effective mechanical support to the infarcted myocardium, thereby promoting favorable tissue remodeling and enhancing functional recovery after MI. (b) A 3D-printed PGS-PCL scaffold exhibiting a multilayered architecture. (c) Young's modulus of various materials determined through tensile testing, illustrating differences in mechanical stiffness (poly-(glycerol sebacate) (PGS)), (poly-(ε-caprolactone) (PCL)). Reproduced with permission from Ref. [69], © WILEY-VCH Verlag GmbH & Co. KGaA, Weinheim 2019. (d) Schematic representation of the microfluidic chip-based fabrication process for anisotropic fibers and total internal reflection fluorescence microscopy (TIRFM) images showing their aligned structure. Reproduced with permission from Ref. [16], © Wiley-VCH GmbH 2024. (e) Underwater rinsing, the CPAMC hydrogel still adhered tightly to the porcine heart, suggesting that this material has good adhesion performance. (f) Schematic illustration of GSH-triggered dissociation of CPAMC hydrogel, demonstrating its complete and controllable detachment behavior. (g) The adhesion properties of three types of hydrogels. (h) Quantitative comparison of adhesive and mechanical properties of CPAMC hydrogels on glass in air with different contact durations. CPAMC: C, aldehyde cellulose (CNC-CHO); P, polyethylenimine (PEI); A, acrylic acid; M, 3-sulfonic acid propyl methyl acrylic acid potassium (MASEP); C, caffeic acid (CA). (i) Echocardiographic images of the left ventricle show that CPAMC treatment significantly increased ventricular wall thickness compared with the MI group, indicating improved myocardial structural recovery. (j) Masson trichrome staining revealed markedly reduced fibrotic tissue (blue) and preserved myocardial tissue (red) in the CPAMC-treated group compared with the MI group, indicating effective attenuation of post-infarction fibrosis. Reproduced with permission from Ref. [85], © He, Y. T. et al. 2022 (panel (a) was created with BioRender.com.)

Cardiac repair materials must provide appropriate mechanical support to mitigate pathological remodeling and restore ventricular function. Among the various mechanical parameters, stiffness and elasticity are primary determinants of myocardial repair efficacy and load-bearing performance [65]. Precise mechanical tuning of myocardial repair materials is primarily achieved by modulating polymer composition and crosslinking density, thereby enabling controlled adjustment of Young's modulus to match native myocardial mechanics [66]. For instance, Efraim et al. fabricated hydrogels with tunable stiffness by integrating decellularized porcine cardiac ECM with varying chitosan content, demonstrating preserved cardiac function and reduced infarct damage in treated models [59]. Moreover, chemical modification enables greater refinement of mechanical properties. Injectable GelMA hydrogels, with Young's modulus adjustable to 14–18 kPa via methacryloyl substitution, combined with miR-222-engineered exosomes, were shown to activate YAP-mediated mechanotransduction and excitation, contraction coupling, thereby enhancing ventricular performance and suppressing fibrosis [67]. Advanced fabrication techniques such as electrospinning and 3D printing further expand the potential for mechanical optimization. Electrospun single-layer (SL) and double-layer (DL) polyurethane (PU) nanofibers exhibit tunable Young's moduli of 74–172 kPa and tensile strengths up to 9.9 MPa, providing structural reinforcement for infarcted myocardium [68]. Similarly, 3D-printed poly(glycerol sebacate)-poly(ε-caprolactone) (PGS-PCL) hybrid scaffolds with a Young's modulus of ~ 748 kPa and tensile strength of ~ 302 kPa alleviated ventricular wall thinning, reduced infarct size, promoted angiogenesis, and decreased cardiomyocyte apoptosis by enhancing M2 macrophage recruitment *in vivo* (Figs. 3(b) and 3(c)) [69]. Beyond stiffness regulation, elasticity is equally crucial for cardiac contraction-relaxation dynamics [70]. Elastin-based biomaterials, for example, have demonstrated remarkable therapeutic potential: pro-elastin significantly reduced scar area and improved contractility in MI rat models, with elevated expression also observed in human ischemic myocardium, suggesting strong translational relevance [29]. Moreover, nano/microstructural design can further enhance material functionality. Electrohydrodynamic (EHD)-printed serpentine PCL stents with 20% elastic deformability closely mimic natural cardiac strain and promote synchronous cardiomyocyte contraction and maturation [71]. Similarly, coaxially electrospun poly(CL-co-TOSUO)/collagen scaffolds exhibit mechanical compliance suitable for cyclic cardiac deformation and effectively deliver mesenchymal stem cells (MSCs), improving cardiac function, enhancing cardiomyocyte survival, and stimulating angiogenesis in MI models [72]. In summary, optimizing the mechanical properties of cardiac repair materials through composition tuning, chemical modification, and advanced manufacturing techniques enables the creation of a controllable biomechanical microenvironment that supports cardiac motion, enhances cellular function, and significantly improves myocardial repair outcomes.

Anisotropic engineering constitutes another essential module in mechanical construction, aiming to reproduce the directional stress distribution of native myocardium. The natural myocardium exhibits pronounced mechanical anisotropy between the longitudinal and transverse directions, with an anisotropy ratio typically ranging from 1.9 to 3.9 [73]. Therefore, beyond optimizing material stiffness and elasticity, introducing anisotropic design is essential to achieve better integration with host tissue and maintain synchronous contractile function. Different degrees of anisotropy can be achieved by tuning the material's composition, concentration, or microstructural organization. Collagen scaffolds with anisotropic fiber alignment more accurately replicate the natural deformation of the epicardium than isotropic counterparts. At the same time, suture fixation enhances the mechanical compliance of the patch compared with adhesive fixation [74]. Similarly, anisotropic polyurethane porous scaffolds fabricated via thermally induced phase separation (TIPS) exhibit mechanical properties closely matching those of native myocardium. When further integrated with decellularized myocardial ECM, the resulting biohybrid scaffold demonstrated superior cell permeability, reduced immunogenicity, and excellent mechanical stability, showing strong potential as a biodegradable patch for MI repair [75]. In addition, advanced fabrication techniques, including beam-scanning SL [76], bioprinting [77], and microfluidic engineering [16], enable precise control over anisotropic microarchitectures. For instance, by introducing alginate, methacrylated gelatin, silver nanowires, and photoinitiators into microfluidic channels and applying controllable shear forces during ion photo-crosslinking, researchers fabricated silver nanowire-reinforced anisotropic hydrogel fiber patches (FP-AA). *In vitro* studies revealed that these patches guided cardiomyocytes to adopt an elongated, oriented morphology resembling that of native myocardium (Fig. 3(d)) [16]. Furthermore, the outward-expanding microneedle (OEBMN) system achieves epicardial self-anchoring and provides multidirectional mechanical reinforcement, significantly increasing ventricular wall thickness, reducing fibrosis, and promoting angiogenesis. Building on this design, the anisotropic microneedle patch (AMP) with a honeycomb microarchitecture exhibited myocardial-matched anisotropic mechanics in a rat MI model, effectively improving ejection fraction, shortening QRS duration, and reducing inflammation and fibrosis by inhibiting MAPK and mTOR signaling pathways, highlighting its clinical translation potential [61]. To quantitatively assess anisotropic performance, experimental characterization methods have also been developed. Using an isolated Langendorff-perfused heart model combined with optical imaging and digital image correlation analysis, researchers evaluated the mechanical response of collagen scaffolds attached to the epicardium. Results demonstrated that anisotropic scaffolds with aligned pores most effectively reproduced the native epicardial deformation pattern. This platform not only quantifies scaffold compliance but also provides a versatile framework for guiding the optimization of anisotropic material design [78].

Adhesion engineering represents a pivotal aspect of mechanical integration, enabling stable epicardial fixation under dynamic cardiac motion while preserving tissue integrity. While achieving anisotropic mechanical matching, most cardiac repair materials still lack inherent adhesion and typically require suturing for fixation. However, suturing can compromise the material's intrinsic mechanical integrity and increase the risk of detachment [79–81]. Moreover, it may exacerbate cardiac injury, leading to adverse effects such as edema, inflammation, bleeding, and even infection. Therefore, endowing cardiac patches with moderate, controllable adhesive properties is of great significance for clinical applications. Current design strategies for adhesion regulation can be broadly categorized into physical fixation and chemical bonding. With the aid of advanced manufacturing technologies such as 3D printing and electrospinning, adhesion strength and distribution can also be

precisely controlled during material fabrication. However, conventional suturing is prone to causing local stress concentration and tissue damage, which has accelerated the development of suture-free fixation strategies. In terms of physical fixation, microneedle patches have gained considerable attention because they can be directly anchored to the epicardium. Early smooth conical microneedles exhibited limited fixation capability, whereas recent biomimetic designs have greatly enhanced anchoring performance. For instance, self-interlocking microneedles inspired by bee stingers achieve strong fixation with minimal penetration depth [82]. Similarly, OEBMN and its optimized AMP provide multidirectional mechanical support while mitigating fibrosis and inflammation, ultimately improving cardiac function in rat models [61]. The chemical bonding strategy focuses on introducing reactive functional groups to strengthen the interactions between the material and the myocardial surface. High-selectivity adhesion can be achieved by forming multiple covalent or non-covalent interactions between dopamine or muscle-derived catechol groups and tissue interfaces [83]. Furthermore, Janus hydrogels with asymmetrical structures exhibit strong adhesion exclusively on the epicardial side. At the same time, the outer layer prevents adhesion to the chest wall or pericardium, thereby preserving both functional performance and surgical safety (Figs. 3(e)–3(h)) [84, 85]. Meanwhile, benefiting from its tunable mechanical properties, the material, after being implanted into rats for 4 weeks, significantly promoted ventricular wall thickening, enhanced cardiac ejection fraction, and reduced fibrosis area, demonstrating excellent myocardial repair efficacy (Figs. 3(i) and 3(j)) [85]. Meanwhile, 3D printing and electrospinning have provided new avenues for constructing adhesive cardiac patches. Adhesive tissue-engineering scaffolds (ATES) printed with self-adhesive bioinks based on tyramine-modified hyaluronic acid and GelMA exhibit excellent mechanical strength and biocompatibility. These patches adhere stably to the myocardial surface and maintain reliable fixation in mouse MI models [86]. In another approach, Zhang et al. developed a double-layer Janus patch via electrospinning. The inner layer, co-electrospun from GelMA and zinc oxide nanoparticles and modified with tannic acid, displayed outstanding mechanical performance, adhesion strength, and antioxidative, anti-inflammatory, and antibacterial properties. The outer layer, composed of poly (L-lactic acid) fibers, effectively prevented exogenous cell invasion and reduced undesired tissue adhesion [87]. By contrast, the Janus structure of GRAXe is established through sequential crosslinking, involving $Ca^{2+}$-induced pre-gelation (trigger A) followed by spatially directed ultraviolet (UV) fixation (trigger B), leading to the formation of an asymmetric interpenetrating ionic-covalent network. This gelation paradigm enables precise spatial control over interfacial network assembly: on the myocardium-contacting side, a highly adhesive anchoring interface is established via MXene-enhanced catechol coupling, whereas the opposite side forms an anti-adhesive surface through dense polymer entanglement, resulting in a 60–150-fold adhesion contrast between the two interfaces. As a result, the material achieves stable *in situ* fixation while effectively reducing the risk of postoperative tissue adhesion [64].

In summary, the regulation of cardiac patch adhesion has evolved from traditional suturing to diversified strategies encompassing chemical modification, biomimetic microneedles, and advanced manufacturing techniques such as 3D printing and electrospinning. These innovations enable stable epicardial anchoring while minimizing tissue damage and preserving anisotropic structural integrity, significantly enhancing the feasibility of clinical translation. Beyond providing mechanical reinforcement and stable fixation, the ultimate goal of myocardial repair lies in restoring electrical coupling and synchronous contractile function in the damaged tissue. Therefore, regulating the electrical conductivity of biomaterials to promote effective signal transmission and coordinated excitation-contraction behavior has emerged as another critical direction in MI repair.

## 3.2 Electrical materials for restoration of cardiac conduction

### 3.2.1 *Evolution of electrical materials for myocardial repair*

Electrical dysfunction after MI primarily arises from disrupted impulse conduction and impaired intercellular coupling, ultimately increasing the risk of myocardial desynchrony and arrhythmia [88]. Therefore, the primary goal of electroactive biomaterials is not merely to enhance tissue conductivity but to reconstruct physiologically relevant electrophysiological structures.

Early conductive systems focused on restoring electrical continuity within the infarcted region by incorporating intrinsic conductive polymers, such as polypyrrole (PPy), polyaniline (PANI), and poly(3,4-ethylenedioxythiophene) (PEDOT) into hydrogels or scaffold matrices [89, 90]. This stage primarily emphasized bulk conductivity enhancement rather than structural precision. Although electrical coupling was improved, the resulting materials often exhibited brittleness and mechanical mismatch with native myocardium [90]. To meet increasing demands for conductivity efficiency and stability, carbon-based nanomaterials, including carbon nanotubes (CNTs), graphene, and their derivatives, have been incorporated into tissue engineering platforms due to their excellent electron-transport properties and high surface areas. These composites markedly enhance intercellular electrical signal propagation and promote the expression of the gap junction protein Cx43, thereby improving the synchronous contraction of cardiomyocytes [13, 88]. However, challenges such as long-term biosafety, uniform dispersion, and stability under dynamic cardiac conditions limit their standalone application [91, 92]. To balance conductivity, bioactivity, and microenvironmental regulation, metal nanoparticles (e.g., gold nanoparticles, AuNPs) and two-dimensional nanomaterials (e.g., MXene) have been increasingly utilized in myocardial repair systems [93, 94]. These materials not only form efficient conductive pathways but also enhance intercellular junction formation and promote angiogenesis by modulating interfacial charge distribution and protein adsorption [95]. Nevertheless, the increasing complexity of these systems introduces new challenges for clinical translation.

It is noteworthy that native myocardium exhibits pronounced anisotropic conductivity, with longitudinal conduction significantly faster than transverse [61]. Restoring global conductivity alone is insufficient for functional reconstruction. Consequently, anisotropic electrical regulation has become a central design principle for myocardial conductive materials [13]. Researches increasingly focus on replicating the anisotropic properties of the myocardial electrical microenvironment. With growing recognition of myocardial electrical anisotropy, advanced fabrication techniques including 3D printing, electrospinning, directional freezing and micropatterning, have enabled the development of directionally conductive

architectures that integrate anisotropic electrical transport with mechanical compliance [31, 96, 97]. This marked the transition from conductivity augmentation to electrophysiological reconstruction. Furthermore, intelligent conductive hydrogel platforms have been developed to support not only enhanced myocardial synchronous contraction but also real-time electrical signal monitoring and tissue repair [98].

Overall, the evolution of electroactive materials in myocardial repair has progressed from simple conductivity enhancement to anisotropic electrophysiological reconstruction, and then to multifunctional microenvironment-responsive systems. This material evolution, which clarifies the mechanisms governing electrical signal propagation at cellular and tissue scales, positions the precise regulation of electrophysiology as a core objective for future research. Accordingly, the next section focuses on conductive network construction strategies that enable controlled signal propagation and anisotropic electrophysiological regulation.

#### *3.2.2 Conductive network design for enhanced electrical signal propagation*

Electrical signals play a pivotal role in MI repair by coordinating excitation-contraction coupling and tissue-level synchronization; following MI, disrupted impulse propagation leads to asynchronous contraction and arrhythmogenic risk. Building on these platforms, recent research has increasingly focused on optimizing the electrical functionality of cardiac tissues through material design, including the incorporation of conductive components or the construction of anisotropic conductivity structures to improve the cardiac microenvironment and promote functional recovery. From a materials engineering perspective, conductive network design in cardiac scaffolds can be broadly categorized into two principal strategies: (i) bulk conductivity enhancement and (ii) anisotropic conductive architecture construction (Fig. 4(a)).

The most fundamental strategy for conductive network construction involves incorporating electrically active components into scaffold matrices to establish percolated conductive pathways within the infarcted region [99]. In cardiac tissue engineering, commonly used conductive biomaterials include carbon-based nanomaterials (such as CNTs and graphene), transition metal carbides (MXenes), conductive polymers (e.g., PPy, PEDOT, and polyaniline), as well as metal nanoparticles (such as AuNPs) [13, 89]. These materials form interconnected conductive networks that restore electrical continuity and enhance intercellular coupling. For example, by *in situ* polymerizing PPy on the surface of silk fibroin (SF) scaffolds, researchers constructed porous conductive scaffolds (SP50) that, when combined with electrical stimulation and cardiomyocytes, formed electroactive engineered cardiac patches (SP50 ECP) with improved excitability and conductivity [100]. Similarly, PPy was grafted onto gelatin to form a water-soluble conductive component (GP), which was then incorporated into oxidized xanthan gum/gelatin hydrogels to create injectable, self-healing OGGP3 hydrogels. These hydrogels not only enhanced conductivity but also improved myocardial signal transmission and angiogenesis [101]. Although PPy exhibits excellent electrical conductivity, its poor solubility and brittleness limit direct biomedical applications; thus, grafting or composite modification is often required to enhance injectability and biocompatibility. In contrast, two-dimensional $Ti_3C_2T_x$ MXene nanosheets have been incorporated into gelatin/dextran aldehyde (Dex-Ald) or silk fibroin-hyaluronic acid (SF-HA) hydrogels to fabricate conductive cardiac patches. These systems significantly improved both the electrical conductivity and myocardial tissue-like elasticity of the hydrogels, while optimizing mechanical strength and adhesion through precise control of MXene concentration (Figs. 4(b) and 4(c)) [93, 102]. However, excessive MXene loading may compromise uniformity and *in vivo* stability, necessitating careful dosage regulation. Moreover, introducing AuNPs into alginate/fibrin (Alg/Fib) hydrogels, in combination with adipose-derived MSC exosomes (Exo) and catalase (CAT), led to the construction of Exo/Hydro/AuNPs/CAT injectable conductive composite hydrogels [103]. AuNPs not only enhanced electrical conductivity but also synergized with biological cues to ameliorate hypoxia and promote myocardial repair, although potential cytotoxicity and dispersion uniformity remain design concerns (Figs. 4(d) and 4(e)) [104, 105]. Overall, these conductive biomaterials can achieve electrical properties approaching those of native myocardium, thereby facilitating effective signal propagation and synchronized cardiomyocyte contraction. Nevertheless, homogeneous conductivity enhancement alone is insufficient to recapitulate the intrinsic anisotropic conduction characteristics of native cardiac tissue.

Notably, native myocardium exhibits significant electrical anisotropy, with the conduction velocity along the fiber axis being approximately three to four times higher than that in the transverse direction, accompanied by marked differences in both longitudinal and transverse conductivities [106, 107]. Therefore, reconstructing directionally dependent conductive pathways has become a critical engineering strategy for restoring physiologically relevant electrical signal propagation in infarcted myocardium. Based on current fabrication methodologies, anisotropic conductive architectures are generally constructed through two complementary approaches: (i) inducing directional alignment of polymer matrices and (ii) regulating the spatial orientation of conductive fillers [108, 109]. Accordingly, common fabrication strategies include mechanical stretching, directional freezing, electrospinning alignment, and related alignment techniques [108, 110, 111]. Meanwhile, researchers introduced highly ordered cellulose nanocrystal (CNC) micropattern structures onto the surface of hydrogels, providing a directionally aligned substrate for cardiomyocyte culture. This design enabled cardiomyocytes to adhere, grow, and align along the patterned direction, thereby recapitulating the anisotropic structural organization of native myocardium (Fig. 4(f)) [112]. These findings further underscore that directional electrical regulation, rather than mere bulk conductivity enhancement, is essential for reconstructing the myocardial electrophysiological microenvironment. Recent studies have begun applying anisotropic conductive materials to MI repair. For example, an anisotropic rGO/SF patch, prepared by integrating reduced graphene oxide with silk fibroin, maintained stable fiber alignment and directional electrical conduction owing to the flexibility and self-assembly properties of silk fibroin [113]. Likewise, a 3D-printed $Ti_3C_2T_x$ MXene-PEG composite scaffold achieved directionally aligned conductive networks through controlled microstructural orientation, effectively guiding cardiomyocyte alignment and enhancing electrical coupling and synchronous contraction [114]. Furthermore, a fiber-filled hydrogel ink printing approach utilized shear forces during extrusion to induce fiber orientation, recent studies have begun applying anisotropic conductive materials to MI repair. For example, an anisotropicrGO/SF patch, prepared by integrating reduced graphene oxide with silk fibroin, maintained stable fiber alignment

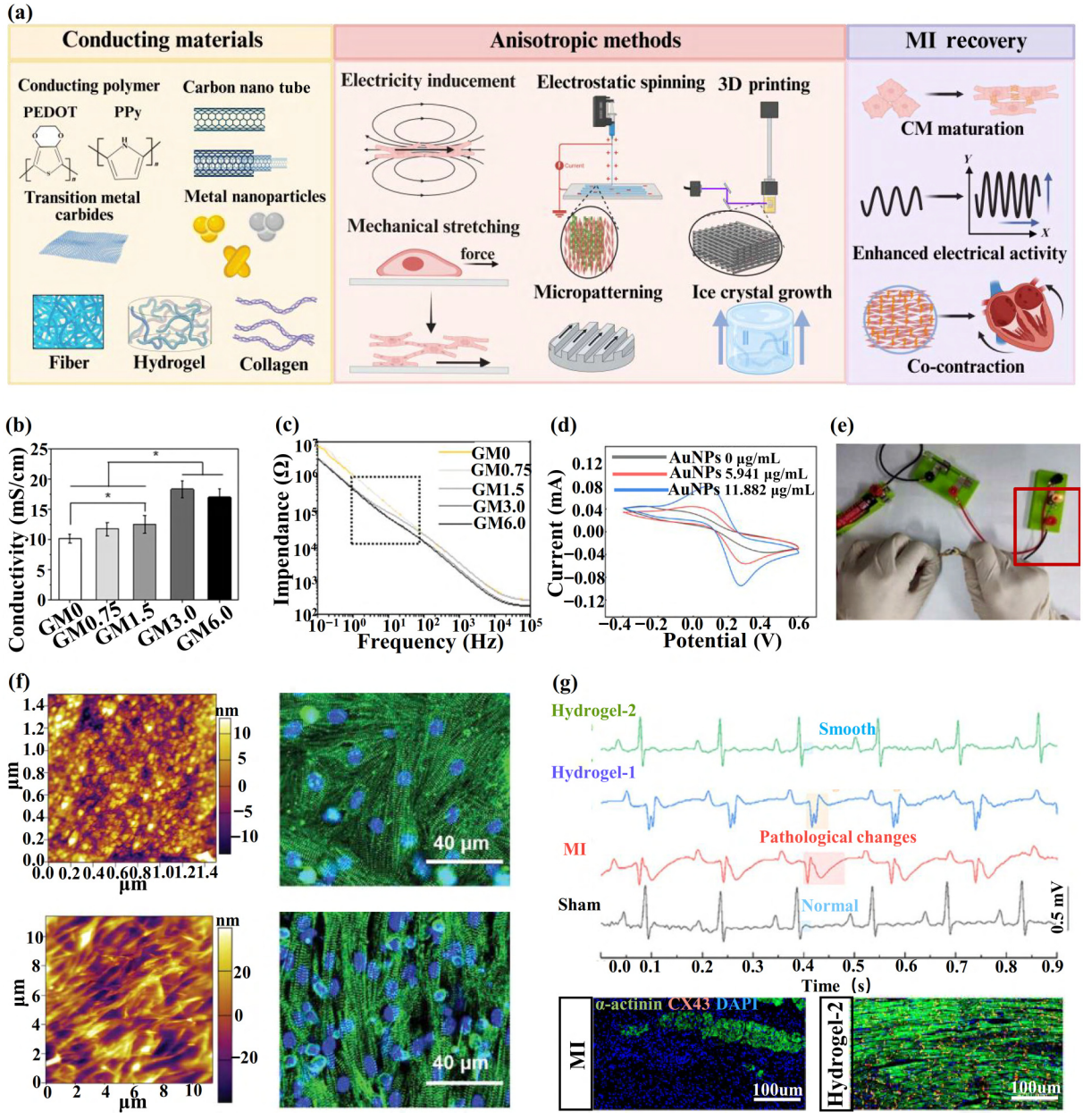


**Figure 4** Electrical regulation restores myocardial signal transduction. (a) By incorporating conductive components (such as conductive polymers, carbon nanomaterials, and metal nanoparticles) to enhance the overall conductivity and integrating external stimuli with tissue engineering approaches to regulate directional electrical conduction, functional materials with anisotropic electrical conductivity can be constructed. These materials help to optimize the post-infarction myocardial microenvironment, promote cardiomyocyte maturation and electrical coupling, and ultimately facilitate cardiac functional recovery. (b) Electrical conductivity was modulated by adjusting the concentration of the incorporated MXene. (c) Resistivity characteristics of materials with different MXene concentrations. Different groups indicate the addition of MXene at different concentrations. Titanium carbide ($Ti_3C_2T_x$) MXene with natural biocompatible polymers (i.e., gelatin and dextran aldehyde (dex-ald)). Reproduced with permission from Ref. [93], © American Chemical Society 2023. (d) Electrochemical performance of HAMA containing different concentrations of AuNPs revealed by cyclic voltammetry (hyaluronic acid methacrylate (HAMA)). (e) HAMA containing AuNPs exhibits higher conductivity, leading to brighter bulb illumination. Reproduced with permission from Ref. [104], © American Chemical Society 2024. (f) AFM images and 2D WAXD patterns reveal the anisotropic structural characteristics of GelMA and micropatterned hydrogel films. Immunofluorescence staining shows that the anisotropic microtopography effectively guides cardiomyocytes to align and grow along the patterned direction, promoting organized, tissue-like morphology. Reproduced with permission from Ref. [112], © Wiley-VCH GmbH 2022. (g) Representative electrocardiograms and α-actinin/CX43 immunofluorescence images of different groups after 28 days of treatment (hydrogel-1: without MXene@PDA; hydrogel-2: containing 1.0% MXene@PDA). Composite hydrogel formed by integrating hydroxypropyl cellulose (HPC) and MXene@PDA nanoconductive materials into a sodium alginate hydrogel network. Reproduced with permission from Ref. [98], © Wiley-VCH GmbH 2025 (panel (a) was created with BioRender.com).

and directional electrical conduction owing to the flexibility and self-assembly properties of silk fibroin. In a rat MI model, this patch outperformed both non-conductive and isotropic conductive controls, significantly improving cardiac pumping efficiency, enhancing cardiomyocyte survival, reducing arrhythmogenic risk, and promoting capillary formation. The resulting engineered tissue exhibited layered contraction behavior closely resembling that of the native heart under electrical stimulation [96]. Furthermore,

researchers have developed a bioinspired hydrogel with both conductivity and structural color features, capable of achieving dynamic monitoring and therapeutic MI repair. By mimicking the conductive network of native myocardium, this hydrogel effectively restored electrocardiogram (ECG) signals and significantly upregulated the expression of connexin Cx43, thereby enhancing intercellular electrical coupling and synchronized contraction while improving overall cardiac electrical conduction. As an intelligent theranostic platform integrating both diagnostic and therapeutic functions, this system provides a promising biomimetic material strategy for functional reconstruction after MI (Fig. 4(g)) [98, 115].

Collectively, anisotropic conductive network construction represents an advanced structural engineering strategy that more faithfully recapitulates the directional electrophysiological characteristics of native myocardium compared with isotropic conductivity enhancement. Looking ahead, by integrating advanced structural control strategies such as 3D printing [96, 116], microfluidics [16], electrospinning, and micropatterning technologies [112], it will be possible to achieve even higher-precision regulation of microstructure and conductive network architecture, thereby providing innovative and effective solutions for MI repair.

### 3.3 Integrated materials for coordinated mechanical and electrical function

#### *3.3.1 Development of mechanically and electrically integrated materials*

Building upon the staged evolution of mechanically and electrically functional biomaterials, it has become increasingly evident that optimizing a single parameter is insufficient to recapitulate the intricate force-electrical coupling of native myocardium. Early material design strategies primarily focused on either mechanical reinforcement of the infarcted myocardium or enhancement of bulk electrical conductivity, without fully integrating mechanical and electrophysiological regulation [117, 118]. However, myocardial infarction simultaneously compromises mechanical integrity and electrical continuity, highlighting the inherent limitations of single-function repair strategies. Consequently, the coordinated reconstruction of both mechanical scaffolds and conductive networks has progressively emerged as a central objective in the developmental trajectory of integrated myocardial repair materials.

In the initial phase of integration, researchers attempted to restore electrical conductivity within mechanically supportive matrices by incorporating conductive fillers, thereby achieving partial electrical compensation in the infarcted region. While such approaches could moderately improve myocardial contraction synchrony, they often neglected the critical interplay between electrical conductivity and mechanical properties, resulting in materials that exhibited additive rather than truly synergistic force-electricity behaviour [45, 119]. This stage thus represents an early, transitional step in the evolution toward integrated mechanoelectrical biomaterials. With a deeper understanding of cardiac force-electrical interactions, the field gradually shifted from simple conductivity enhancement to coordinated dual-parameter regulation. Composite strategies combining functionalized conductive polymers, metallic or carbon-based nanoparticles, and tunable hydrogels have enabled simultaneous modulation of mechanical properties and electrical conductivity, achieving an initial level of force-electricity synergy approaching the physiological range of native myocardium [13, 102, 120]. For example, CNT-GelMA hydrogels and PPy-gelatin composite hydrogels maintain flexible mechanical properties while exhibiting stable electrical conductivity, thereby providing enhanced support for synchronized cardiomyocyte contraction [47, 121].

More recently, force-electricity co-design has evolved into a structure-level regulatory framework. Advanced manufacturing techniques have enabled the creation of controllable composite systems that provide tailored mechanical support [122–124]. Notably, PGS-CNT anisotropic elastic conductive patches and gold-plated serpentine fiber scaffolds not only reproduce ventricular wall elasticity and electrical conductivity but also guide cardiomyocyte orientation through structural design, enhancing both electrical signal synchrony and pumping efficiency [71, 125]. Concurrently, the importance of the infarct microenvironment in stabilising force-electrical synergy has become increasingly evident. Functionalization strategies are now being integrated with microenvironmental responsiveness: reactive oxygen species (ROS) scavengers, pH-buffering components, and anti-inflammatory factors are incorporated to achieve simultaneous force-electrical modulation within the pathological milieu [71, 126]. These dynamic composite hydrogels not only provide mechanical and electrical support but also enhance cell survival, mitigate fibrosis, and promote angiogenesis, offering a more comprehensive, multifunctional approach to myocardial repair [127].

Overall, although force-electricity synergy materials have shown continuous performance improvements, current design strategies largely remain focused on single-dimensional enhancements, lacking a unified framework for multi-parameter coupling. As understanding of myocardial force-electrical synergy deepens, the emphasis is shifting from incremental performance optimization toward integrated, multidimensional regulation of both mechanical and electrical properties.

#### *3.3.2 Construction of composite systems for mechanical-electrical coordination*

At present, the construction of mechanoelectrical coordinated systems for MI repair primarily revolves around two foundational design objectives: (i) matching the elastic modulus and mechanical compliance of native myocardium through matrix composition optimization and crosslinking regulation, and (ii) enhancing electrical conductivity via incorporation of conductive polymers, metallic nanoparticles, or carbon-based nanomaterials. While these approaches have yielded promising improvements in structural reinforcement or signal transmission, they often remain parameter-oriented and insufficient to fully reconstruct the intrinsic force-electrical coordination of cardiac tissue. Therefore, the strategic construction of composite systems that integrate mechanical adaptability with conductive continuity has emerged as a central design paradigm for next-generation myocardial repair materials (Fig. 5(a)).

The most straightforward construction strategy involves reinforcing natural or synthetic hydrogel matrices with conductive fillers to simultaneously improve stiffness and electrical conductivity [128, 129]. The incorporation of conductive fillers enhances both the mechanical and electrical properties of natural hydrogel systems. For example, a composite hydrogel composed of CNTs and GelMA exhibits an elastic modulus of approximately 16.8 kPa, while the action potential duration of CNT-GelMA

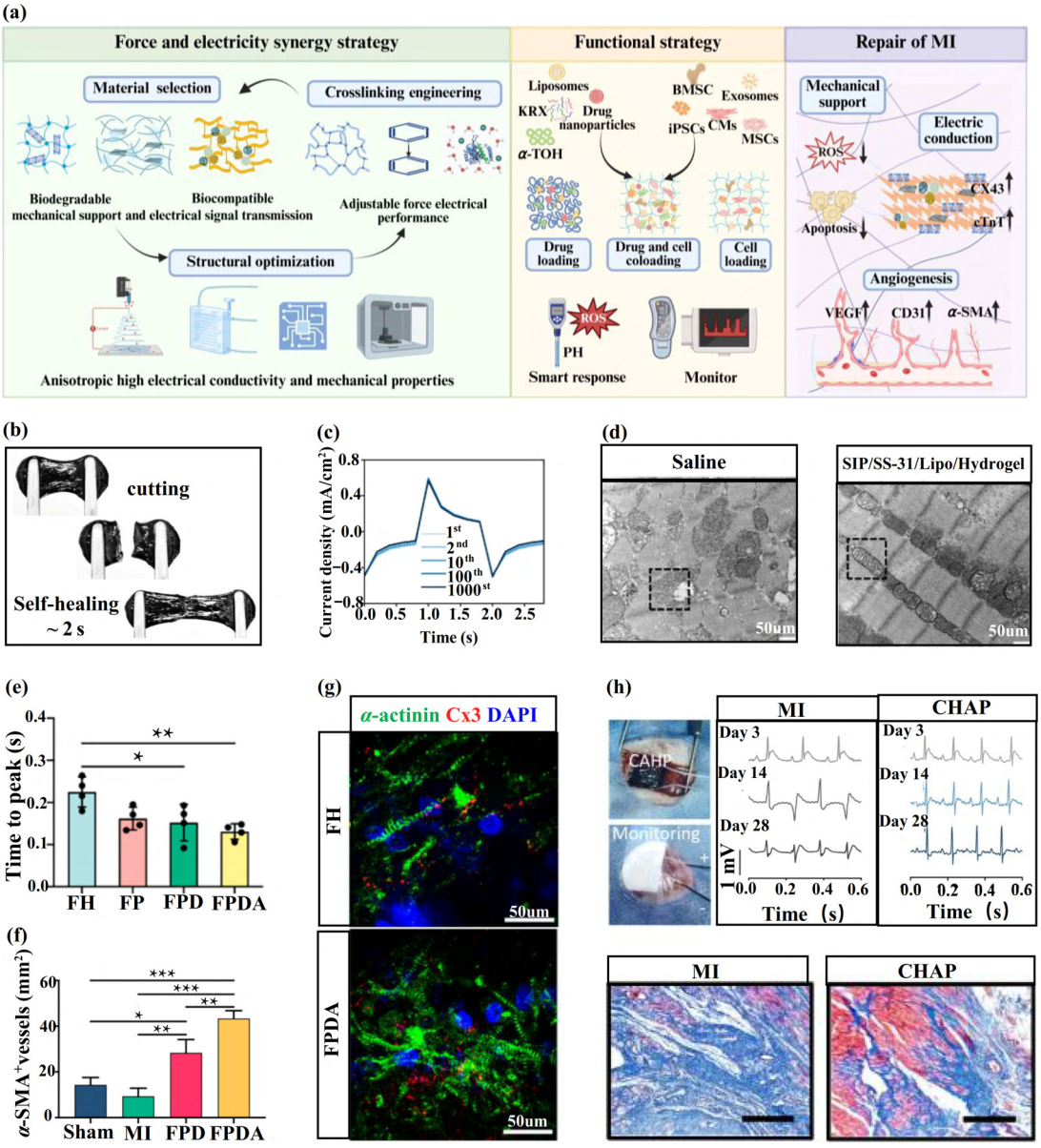


**Figure 5** The synergy of force and electricity promotes MI repair. (a) By integrating mechanically and electrically tunable functional materials with tissue engineering approaches to achieve structural adaptability, the requirements for force-electrical coordination and tissue reconstruction in MI repair can be effectively addressed. Furthermore, incorporating multifunctional strategies, such as drug and/or cell loading, and introducing intelligent stimuli-responsive systems sensitive to ROS and pH enables real-time monitoring of the repair process while further enhancing myocardial regeneration and functional recovery. (b) The MEHPs possess tensile properties and can self-heal within 2 s. (c) The 1000 charge-discharge cycles demonstrate that MEHP exhibits excellent electrochemical stability under physiological conditions. Reproduced with permission from Ref. [130], © American Chemical Society 2022. (d) TEM images show that the mitochondrial morphology was repaired after the material treatment. elamipretide (SS-31), sphingosine-1-phosphate (S1P). Reproduced with permission from Ref. [126], © Wiley-VCH GmbH 2022. (e) Compared with other material groups, the FPDA treatment group reached the calcium ion peak in the shortest time. (f) FPDA promotes angiogenesis in the infarct. (g) Immunofluorescence analysis of the expression of α-actin (green) and connexin 43 (Cx43, red) in myocardial cells under the action of different hydrogels. FH was defined as F127DA hydrogel and FP was defined as FH mixed PEDOT: PSS, FPD was defined as FP mixed PDA, and FPDA was FPD hydrogel with α-TOH added. F127DA: polyether F127 diacrylate, PEDOT:PSS: poly(3,4-ethylene dioxythiophene):poly(styrenesulfonate). Reproduced with permission from Ref. [134], © American Chemical Society 2024. (h) The time-programmable adhesive hydrogel patch (CAHP) can firmly adhere to the epicardial surface, enabling continuous electrocardiographic monitoring, while significantly improving cardiac function and reducing fibrosis, thereby demonstrating excellent therapeutic efficacy. Reproduced with permission from Ref. [144], © Yu, C. et al. 2023 (panel (a) was created with BioRender.com).

reaches 0.62 s at 50% amplitude, effectively replicating the electrophysiological characteristics and rhythmic contractions of the myocardium [121]. Although this strategy enhances dual properties concurrently, mechanical and electrical regulation are still primarily achieved through additive reinforcement rather than intrinsic coupling.

To overcome the limitations of additive reinforcement, a second strategy focuses on constructing dynamically crosslinked conductive networks that intrinsically integrate flexibility, resilience, and electrical conductivity. By combining conductive polymers with reversible chemical bonds, these systems achieve synchronized mechanical adaptability and conductive stability under cyclic

cardiac loading. The injectable MEHP, constructed from self-doped polyaniline-gelatin (b-PANi:Gel) and polyvinyl alcohol (PVA), forms a dynamic network via borate ester bonds and non-covalent interactions. This hydrogel demonstrates high mechanical resilience, myocardium-matched conductivity, and self-healing as well as anti-fatigue properties, maintaining structural and functional stability under continuous cardiac cycles. Moreover, MEHP can be minimally invasively delivered and firmly adhere within the pericardial cavity, forming a tight interface with the infarcted myocardium and enabling highly synchronized force-electrical coupling. Its injectability, tissue adhesion, and dynamic adaptability endow MEHP with significant clinical translation potential, representing a promising minimally invasive mechanoelectrical repair strategy for MI treatment (Figs. 5(b) and 5(c)) [130]. Similarly, an OGDPR hydrogel, constructed via dual crosslinking of xanthan gum and gelatin through imine and borate ester bonds, and incorporating PPy, achieved cardiac tissue-matched electrical conductivity ($6.27 \times 10^{-4}$ S/cm) and elastic modulus (45.35 kPa), leading to substantial improvements in cardiac function and tissue regeneration in MI models [101].

Beyond compositional tuning, a higher-level construction strategy involves engineering multiscale architectures that spatially coordinate mechanical anisotropy and electrical pathways. Advanced manufacturing techniques such as electrohydrodynamic printing, excimer laser microablation, and embedded 3D printing enable precise control over fiber orientation, micro-patterning, and hierarchical porosity. For instance, a gold-coated serpentine ultrafine fiber scaffold fabricated by electrohydrodynamic printing demonstrated approximately 20% elastic deformation, effectively matching myocardial strain. At the same time, the AuNP coating endowed it with excellent electrical conductivity, improving intercellular connectivity and left ventricular remodeling in MI models [71]. Additionally, an AuxCP patch fabricated by excimer laser microablation adopted a honeycomb "bow-tie" micro-pattern, enabling tunable mechanical anisotropy, while its chitosan-polyaniline composite matrix provided stable conductivity, collectively reducing wall stress and maintaining synchronous cardiac beating [131]. Meanwhile, PGS-CNT anisotropic elastomeric conductive patches, fabricated via a melt-based embedded 3D printing platform, achieved close conformity with rat ventricular curvature and mechanical anisotropy through programmable honeycomb microarchitectures. CNT incorporation endowed the patches with favorable mechanical and electrical properties, thereby facilitating synchronized electrical signal propagation and functional recovery in infarcted myocardium [125]. Overall, mechanoelectrically coupled materials exhibit far greater potential than single-function materials by simultaneously providing mechanical support and electrical signal conduction. Their porous structure, excellent biocompatibility, and tunable properties also offer an ideal platform for drug or cell delivery, further enhancing the comprehensive therapeutic efficacy of myocardial repair. During MI repair, mechanical matching and electrical signal conduction provide essential initial structural and functional support. However, long-term recovery depends on reshaping the pathological microenvironment of the infarcted tissue. Excessive ROS accumulation, acidic pH, and persistent inflammation aggravate cell apoptosis and tissue damage. Therefore, beyond electromechanical restoration, materials with ROS-scavenging, pH-buffering, and anti-inflammatory functions are critical for improving cardiomyocyte survival and functional recovery (Fig. 5(d)) [126, 132, 133]. The fluorescent polydopamine (FPDA) hydrogel, composed of depopulated Pluronic F127 micelles as the macroscopic crosslinking network, incorporates conductive components and polydopamine (PDA), and loads the hydrophobic antioxidant $\alpha$-tocopherol ($\alpha$-TOH) to form an injectable, highly compliant antioxidant-conductive composite. *In vitro* and *in vivo* evaluations confirmed that FPDA hydrogel effectively mitigated oxidative stress, induced injury while preserving electrophysiological function, thereby validating the feasibility of integrating antioxidant capacity into conductive scaffolds for synergistic myocardial repair (Figs. 5(e)–5(g)) [134]. Moreover, excessive fibrosis following MI increases ventricular stiffness and disrupts electrical conduction, thereby weakening force-electrical coupling. In addition to providing structural support that mitigates stress-induced fibrosis, fibrosis suppression can be achieved by regulating MMP activity and introducing stem cells [15, 135]. Recent work showed that encapsulating human induced pluripotent stem cell-derived cardiomyocytes (hiPSC-CMs) within hyaluronic acid-based hydrogels doped with AuNPs promoted gap junction formation, enhanced electrical coupling, and leveraged MMP-2 responsive degradation to achieve targeted repair in ischemic myocardium, ultimately reducing fibrosis and promoting angiogenesis [95]. Similarly, alginate (SA)-based composite hydrogels loaded with bone marrow mesenchymal stem cell exosomes (mBMSC-EV) and the PAP peptide effectively modulated the TGF-$\beta$1/SMAD and TRPC6/NFAT signaling pathways, suppressing fibrosis while promoting myocardial regeneration [136]. These strategies demonstrate how mechanoelectrically integrated materials can actively regulate ECM dynamics to preserve conductive continuity. Furthermore, the insufficient blood supply to damaged myocardium critically limits long-term recovery. Thus, integrating pro-angiogenic factors into conductive matrices has emerged as a key strategy. By integrating bioactive factors [137], stem cell secretes [138] or endothelial cells [139]. Such bioactive components, these multifunctional materials can not only provide mechanical support and electrical signal transmission that match natural myocardium, but also promote microangiogenesis, improve microcirculation and enhance the survival and function of myocardial cells. The Gel@CK hydrogel integrates conductive CNTs and angiogenic peptides (KRX) into a natural polysaccharide matrix through electrostatic adsorption, achieving a synergistic improvement in the conductivity, biocompatibility and angiogenic function of the material. It shows significant ROS clearance ability and promotes endothelial cell proliferation and angiogenesis *in vitro*. It significantly improves cardiac function and reduces infarction area [137, 140]. Collectively, these multifunctional composite strategies advance mechanoelectrical coordination from structural compensation toward integrated therapeutic regulation, enabling sustained force-electrical synergy in the infarcted myocardium. To further evaluate and refine the performance of such materials *in vivo*, complementary monitoring strategies have also been explored.

#### 3.3.3 *Integration with electronic devices for functional monitoring*

In MI therapy, effective repair increasingly relies on the integration of therapeutic materials with functional monitoring systems [141]. Although engineered cardiac patches (ECHs) incorporating therapeutic agents or stem cells have shown promising results, continuous tracking of post-intervention cardiac function remains essential in clinical practice to optimize therapeutic strategies and achieve personalized treatment. Recently, a new generation of ionic conductive hydrogel-based cardiac patches have been developed for

the simultaneous real-time monitoring and repair of MI. For instance, a nano-clay composite ion-conducting hydrogel, designed with surface wrinkling and layered structures, exhibits strong protein antifouling ability and precise infarction site detection. The incorporation of amphiphilic sulfamethazine acrylate monomers significantly enhances ion mobility, electrical conductivity, and biocompatibility, enabling the hydrogel to sensitively respond to subtle electrical changes induced by cardiac micro-deformations [142]. Another example is a core-shell curcumin-nanocomposite-reinforced hydrogel coated with PDA, where ionic bonding and proton conduction confer high ionic conductivity, elasticity, and fatigue resistance. This system can discriminate the degree of MI through resistance signal variations, allowing real-time in vivo monitoring [143]. Further progress has been reported with a functionalized polyaniline-based time-programmed adhesive hydrogel patch (CAHP), which achieves spatiotemporally selective adhesion to the dynamic epicardial surface. The patch combines strong adhesive toughness, rapid self-healing capability, and enhanced electrochemical performance. Beyond therapeutic reinforcement, it enables real-time monitoring of systolic and diastolic activity while supporting ventricular remodeling inhibition and angiogenesis through electro-coupling effects (Fig. 5(h)) [144].

Overall, these highly sensitive, conformal ion-conductive hydrogel scaffolds not only achieve effective MI repair *in vivo* but also enable non-invasive, real-time assessment of myocardial status without exacerbating local damage. However, current studies primarily rely on acute MI models in small animals, which are limited by short observation windows, insufficient pathological fidelity, and lack of long-term functional evaluation. Future research integrating advanced *in vitro* platforms, such as cardiac organoids and heart-on-a-chip systems, is expected to provide more accurate models of MI pathophysiology and establish innovative platforms for real-time disease monitoring and therapeutic optimization following material-based interventions.

## 4 Therapeutic effects of force-electrical synergistic materials in myocardial repair

Two-dimensional (2D) cellular models are initially employed to elucidate cytocompatibility, electrical coupling, calcium handling, and Mechan transduction at the single-cell level [145]. However, their simplified architecture and limited multicellular interactions restrict the ability to predict tissue-level remodeling. Three-dimensional (3D) cardiac organoids offer improved physiological relevance by recapitulating spatial organization and ischemia-associated structural responses [146, 147]. Yet they still lack precise control over perfusion, electromechanical stimulation, and real-time functional monitoring. Heart-on-a-chip (HoC) platforms further advance this modeling hierarchy by integrating controlled perfusion, programmable mechanical and electrical cues, and embedded sensing systems, thereby enabling more accurate simulation of the dynamic infarct microenvironment [148, 149]. Nevertheless, *in vivo* animal models remain indispensable for validating long-term therapeutic efficacy, electrical integration, immune modulation, and functional recovery within the systemic physiological context [150, 151].

This progressive transition from simplified *in vitro* systems to whole-organ validation ensures systematic assessment of force-electrical synergistic materials across increasing biological complexity. With the rapid advancement of organoid and organ-on-chip technologies, these human-relevant platforms are expected to complement, and potentially reduce reliance on, animal studies in future myocardial infarction research (Fig. 6(a)) [152, 153].

### 4.1 Promoting cardiomyocyte survival and electromechanical maturation under force-electrical regulation

The *in vitro* biological performance of force-electrical synergistic materials is commonly evaluated using multiple cardiomyocyte models, including rat embryonic cardiomyocytes (H9c2), neonatal rat cardiomyocytes (NRCMs), and hiPSC-CMs. These models enable a multidimensional assessment of material efficacy, including cell viability, sarcomere maturation, gap junction formation, and the restoration of electromechanical coupling [67, 154].

Biocompatibility remains the fundamental prerequisite for myocardial repair materials. Classical concepts emphasize the need to support host tissue integration and maintain cellular function while minimizing inflammation and cytotoxicity [155]. More recent perspectives extend this definition beyond "non-toxicity" toward actively promoting regeneration-supportive microenvironments [156]. Accordingly, current myocardial repair materials often employ high-molecular-weight synthetic polymers and naturally derived matrices with established biocompatibility, such as polyacrylic acid (PAA), PCL, glycerol-based polymers, anedioic acid derivatives, and extracellular matrix-based materials. These systems provide stable adhesion interfaces and appropriate mechanical support, preserve cellular homeostasis, and attenuate inflammatory responses, thereby creating conditions conducive to functional reconstruction [69, 125].

Building on this biocompatible foundation, force-electrical synergistic materials further modulate cardiomyocyte behavior by coordinating mechanical cues with electrical conductivity. Experimental studies demonstrate reduced apoptosis and enhanced proliferation, partly associated with regulation of Bax/Bcl-2 balance, suppression of SIRT1/p53-mediated inflammatory signaling, and activation of mechanotransduction pathways [67, 88, 157, 158]. Improvements in mitochondrial function and cellular energy homeostasis accompany these molecular effects.

Importantly, coordinated mechanical and electrical regulation contributes to cardiomyocyte structural and functional maturation. *In vitro*, studies consistently report enhanced sarcomere organization, increased Cx43 expression, and improved contraction synchronization in conductive or anisotropic scaffolds [89]. For example, hydrogel fiber patches (FP-AA) induce elongated and aligned cardiomyocyte morphology resembling native myocardium, with more organized sarcomere patterns and significantly increased sarcomere length compared to non-conductive controls [16]. Incorporation of conductive networks further enhances Cx43 expression and spatial distribution, as confirmed by flow cytometry and immunofluorescence analyses. Functional measurements demonstrate improved spontaneous contraction regularity, greater synchronization of calcium transients, and enhanced coupling between action potential propagation and contractile amplitude [96, 114, 154].

Collectively, these findings indicate that force-electrical synergistic materials promote cardiomyocyte maturation at both structural and functional levels and partially restore electromechanical coordination *in vitro*, thereby providing a cellular basis for subsequent tissue-level repair after myocardial infarction.

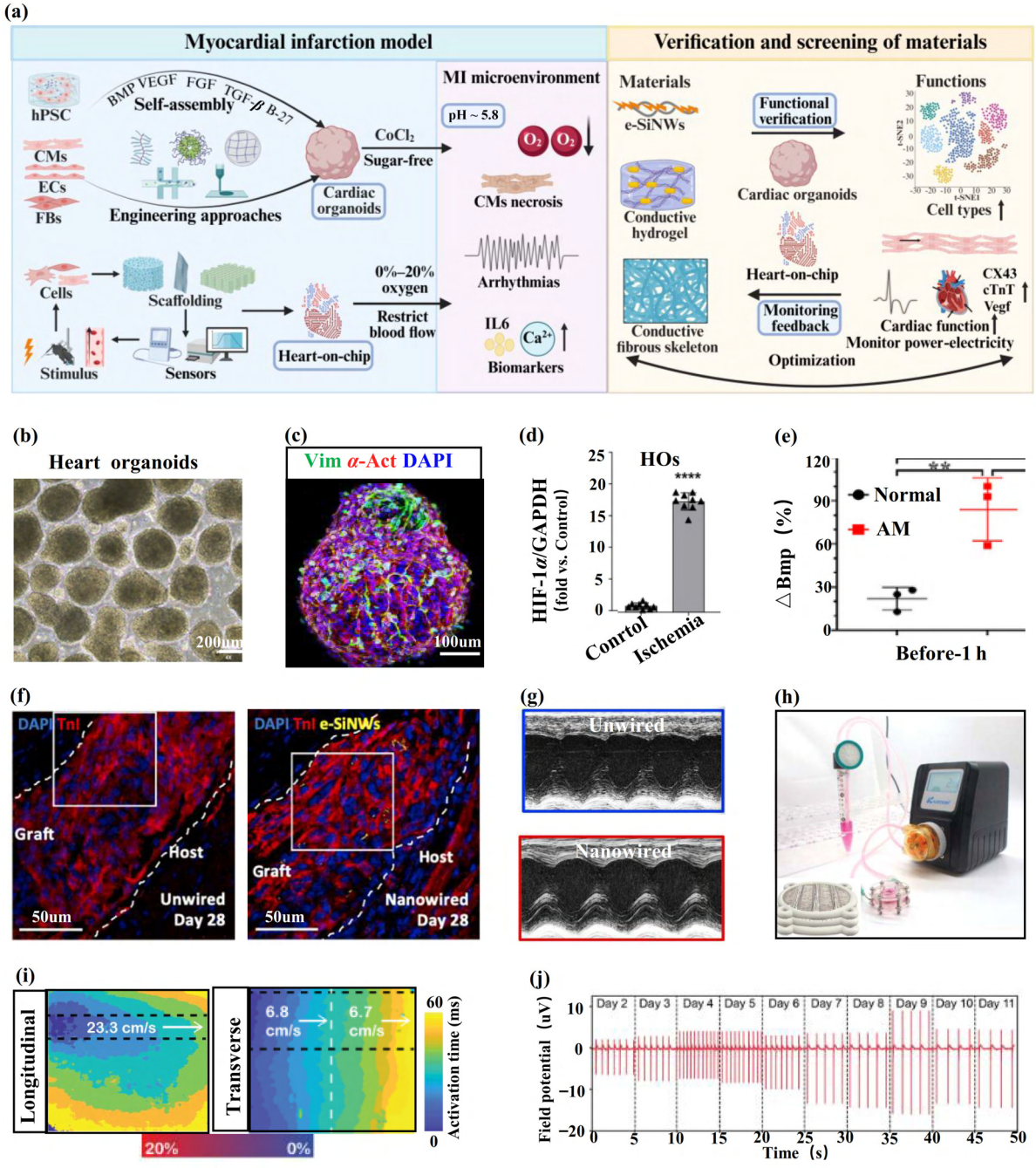


**Figure 6** The Application of cardiac bionic Platform in the research of myocardial repair with force-electrical materials. (a) Cardiac organoids and heart-on-a-chip systems, as advanced *in vitro* models, can replicate MI pathology through various strategies and precisely simulate ischemic and hypoxic conditions by modulating pH and oxygen concentration gradients. Moreover, these bioengineered platforms serve as powerful tools for material screening and therapeutic efficacy evaluation, enabling comprehensive assessment of myocardial repair performance. Leveraging the real-time monitoring capability of organ-on-a-chip technology allows dynamic feedback and optimization of material properties, thereby providing valuable guidance for the rational design and clinical translation of MI repair materials. The image was created with BioRender.com. (b) Bright-field image of HOs. (c) Z-stack image of co-staining in Hos. Vimentin (green) marks fibroblasts, α-actinin (red) marks cardiomyocytes, and DAPI (blue) stains nuclei. (d) Upregulation of hypoxia-inducible factor 1α (HIF-1α) expression under hypoxic conditions after MI. Reproduced with permission from Ref. [166], © Song, M. et al. 2024. (e) Acidic microenvironment (AM) significantly increased the beating frequency of HCOs. Reproduced with permission from Ref. [167], © Wang, F. et al. Advanced Materials published by Wiley-VCH GmbH 2025. (f) Compared with the unwired grafts, the nanowired grafts increased expression of cardiac troponin I (TnI) after 28 days of treatment, indicating enhanced cardiomyocyte functional recovery and improved myocardial repair. (g) Compared with the unwired group, the nanowired group exhibited a reduced left ventricular end-systolic diameter (LVESD) and enhanced cardiac contractile function. Reproduced with permission from Ref. [168], © Tan, Y. et al. some rights reserved; exclusive licensee American Association for the Advancement of Science 2023. (h) Schematic illustration of the cardiac organ-on-a-chip system. Reproduced with permission from Ref. [173], © Wiley-VCH GmbH 2023. (i) In a cardiac organ-on-a-chip model, an oxygen concentration gradient was established to investigate the propagation characteristics and velocity differences of calcium waves in both longitudinal and transverse directions. Reproduced with permission from Ref. [175], © Rexius-Hall, M. L. et al. some rights reserved; exclusive licensee American Association for the Advancement of Science 2022. (j) Real-time monitoring of electromechanical activity over 11 days using the HOC platform to guide material design and promote effective MI repair. Reproduced with permission from Ref. [181], © American Chemical Society 2025.

### 4.2 Modeling myocardial infarction in three-dimensional cardiac organoids to evaluate structural and functional restoration

Human cardiac organoids (hCOs) are three-dimensional multicellular constructs derived from the *in vitro* self-organization of human stem cells. They can partially recapitulate the histological architecture, physiological function, and pathological responses of the human heart, providing a promising platform for investigating cardiac development, disease mechanisms, and therapeutic strategies. Currently, hCOs' construction methods can be broadly categorized into three main approaches: self-assembly, tissue engineering, and 3D bioprinting. enable the generation of multicellular cardiac tissues containing cardiomyocytes, fibroblasts, and endothelial cells [148, 159–161]. For instance, integrating human amniotic epithelial stem cells (hAESCs) with immunomodulatory capacity into porous antioxidant polyurethane (PUR) scaffolds resulted in stem-cell cardiac patches that significantly enhanced angiogenesis, reduced fibrosis, and improved ventricular remodeling and cardiac function [162]. While these approaches differ in controllability and structural precision, they collectively offer reproducible 3D cardiac microenvironments suitable for disease modeling and therapeutic assessment. Importantly, compared with traditional two-dimensional cultures, hCOs better preserve cell–cell interactions, extracellular matrix organization, and synchronized electromechanical activity, making them particularly valuable for evaluating force-electrical synergistic materials [163, 164].

In MI modeling, hCOs can be subjected to hypoxic, ischemic, and acidic microenvironments to reproduce pathological features characteristic of acute MI. Building on established mesodermal differentiation protocols for cardiac organoids [165], pluripotent stem cells were first induced toward the mesodermal lineage. Hypoxic stress induced by $CoCl_2$ and glucose deprivation triggers cardiomyocyte apoptosis, contractile dysfunction, abnormal calcium handling, and altered beating patterns, closely mirroring *in vivo* MI pathology (Figs. 6(b)–6(d)) [166]. Similarly, exposure to acidic conditions (pH ~ 5.8) reproduces post-infarction extracellular acidosis and further exacerbates functional impairment (Fig. 6(e)) [167]. These controllable injury models establish a robust *in vitro* system for assessing structural damage and electromechanical dysfunction.

Importantly, hCOs not only serve as robust *in vitro* platforms for evaluating the function of cardiac repair materials, but also as screening systems to identify materials best suited for MI therapy. For instance, recent studies used hCOs to assess the repair potential of conductive silicon nanowires (e-SiNWs). Incorporating e-SiNWs into organoids containing hPSC-derived cardiomyocytes, fibroblasts, and endothelial cells significantly enhanced electrical pacing, contractile function, and ischemic tolerance. When transplanted into infarcted rat hearts, the nanowire-enhanced organoids promoted superior cell maturation, angiogenesis, and cardiac functional recovery, while mitigating left ventricular remodeling, compared with control organoids. Mechanistically, the enhanced conductivity of e-SiNWs facilitated electrical coupling with host myocardium, evidenced by elevated connexin-43 (Cx-43) expression and long-term tissue integration (Figs. 6(f) and 6(g)) [168].

Collectively, these studies demonstrate that hCOs represent a powerful platform not only for disease modeling and drug discovery, but also for functional evaluation of electromechanically coupled biomaterials in MI repair. Nevertheless, current hCO models still face challenges in precise control of external stimulation, hydrodynamic regulation, and real-time monitoring, underscoring the potential of emerging heart-on-a-chip (HoC) technologies to overcome these limitations and advance translational cardiac research.

### 4.3 Utilizing heart-on-a-chip platforms to recapitulate dynamic cardiac microenvironments and assess therapeutic efficacy

The HoC is a micro-bionic platform that integrates microfluidics, biomimetic scaffolds, and multicellular co-culture systems. It enables the simulation of blood flow and cellular microenvironments through controlled perfusion and allows real-time monitoring of physiological functions and disease progression at the organ level [165, 169]. By enabling controlled perfusion, programmable mechanical and electrical stimulation, and real-time functional monitoring, HoC systems provide a physiologically relevant platform for evaluating the therapeutic efficacy of force-electrical synergistic materials.

Structurally, HoC platforms typically incorporate human induced pluripotent stem cell-derived cardiomyocytes (hiPSC-CMs), fibroblasts, and endothelial cells within PDMS- or PMMA-based microfluidic architectures [170–172]. To better mimic the native ECM, hydrogels such as collagen, gelatin, and methacrylated gelatin (GelMA), as well as conductive polymers, are often incorporated. When combined with electrospinning and 3D bioprinting, these materials can achieve anisotropic architectures with tunable mechanical and electrical properties [116]. For example, by combining 3D printing and electrospinning, researchers have fabricated a three-dimensional anisotropic cardiac scaffold. This design involved the layered assembly of 4D4S scaffold blocks, seeded with cardiomyocytes, and stabilized using GelMA photocrosslinking, resulting in an integrated anisotropic structure. When incorporated into a microfluidic perfusion system, this scaffold formed a 3D anisotropic HoC model, combining the structural precision of 3D printing with the fiber orientation of electrospinning. This hybrid approach not only optimized scaffold architecture but also created an ideal mechanical microenvironment for myocardial cell growth and maturation (Fig. 6(h)) [173]. These features are particularly important for replicating myocardial force transmission and electrical conduction in a controllable setting. Another significant advantage of HoC systems is their ability to support dynamic culture conditions. By applying external electrical stimulation and mechanical stress, HoCs can reproduce the complex electromechanical environment of the native myocardium, thereby greatly enhancing cardiomyocyte structural and functional maturation [174]. For instance, a 3D heart bundle constructed from a fibrinogen-matrix gel composite was integrated into a microfluidic HoC platform. Compared with static culture, this dynamic perfusion system, by providing continuous oxygen supply and nutrient exchange, significantly improved biocompatibility, calcium handling, and contractile performance, while upregulating mature cardiac markers such as α-actinin, α-tubulin, Cx43, and cardiac troponin T (cTnT) [174]. Furthermore, integrating multimodal biosensors enables real-time monitoring and precise regulation of microenvironmental parameters, enabling adaptive feedback control of stimulation conditions. This combination substantially enhances the physiological relevance, stability, and controllability of HoC-based *in vitro* cardiac models [171].

In modeling MI, common strategies involve modulating oxygen concentration and restricting perfusion to mimic the ischemic microenvironment. For instance, a PDMS-based microfluidic chip generating a 0%–20% linear oxygen gradient successfully reproduced key hypoxic pathophysiological features, including calcium handling disorders, reduced contractile stress, and inflammatory responses. This platform effectively replicated the core pathological characteristics of ischemic heart disease, providing a novel tool for studying MI mechanisms and developing therapeutic strategies (Fig. 6(i)) [175]. However, this model primarily focused on the infarct border zone, lacking a representation of the entire infarcted myocardium. To achieve more comprehensive modeling, advanced platforms incorporating hiPSC-derived cardiomyocytes, fibroblasts, and endothelial cells have recapitulated fibrosis, vascular injury, and arrhythmogenic activity under ischemic conditions [176, 177]. Recent co-culture systems integrating macrophages further reproduce inflammatory-cardiac crosstalk, providing a more comprehensive representation of post-MI remodeling [178]. These dynamic injury models establish HoC as a robust platform for evaluating therapeutic interventions under physiologically relevant stress conditions.

Building on this foundation, HoC systems have been further employed to assess the repair potential of mechano-electrical coupling materials. By integrating conductive hydrogel scaffolds with biomimetic hiPSC-derived cardiomyocytes and fibroblasts, these platforms enhance myocardial contractility and electrical signal propagation, offering a robust tool for the screening and functional validation of materials for MI repair. Current HoC models primarily focus on mimicking the pathological microenvironment of MI, while studies on their mechanical and electrical properties remain limited. Conductive and anisotropic hydrogels incorporated into PDMS-based chips guide cell alignment and rhythmic beating while enabling visual or electrical signal readout [179]. Embedding collagen-Matrigel matrices doped with gold nanorods into microfluidic systems further enhances electrical conductivity and contractile performance, providing a controllable platform for optimizing material composition [180]. MI repair requires the synergistic action of mechanoelectrical materials. To achieve mechanical property matching, researchers have employed a "liquid–gas phase transition–induced porosity" technique to introduce a porous structure into PDMS, thereby reducing its Young's modulus to mimic the mechanical characteristics of cardiac tissue (epicardium: 30–70 kPa; soft ECM: 28–37 kPa). During continuous 11-day electromechanical monitoring, this mechanically compliant HoC significantly improved cardiomyocyte function by upregulating genes associated with cell adhesion (ITGA1), contraction (CACNA1C), and electrical signal propagation (SCN5A, KCNH2). Consequently, it enhanced myofibrillogenesis and shortened the ECC delay by approximately 128% (Fig. 6(j)) [181]. Moreover, integrating real-time sensors enables precise monitoring of contractile force and electrophysiological activity, enabling fine-tuned regulation of mechano-electrical characteristics [182]. Emerging techniques, such as laser-assisted EHD printing, enable the fabrication of microfiber scaffolds with embedded microelectronics. These scaffolds promote cell alignment and allow *in situ* electrophysiological monitoring. Such capabilities provide new opportunities for drug testing and organ-on-a-chip applications [183]. Through these advancements, HoC platforms can not only recapitulate the *in vitro* microenvironment of MI but also serve as innovative systems for the screening, functional assessment, and potential clinical translation of mechano-electrical coupling materials.

In conclusion, cardiac organoids and heart-on-a-chip technologies together provide a transformative platform for advancing research and applications of mechano-electrical synergy materials in MI repair [167]. While organoids realistically reproduce tissue architecture and pathological progression, HoC systems offer precise control over shear forces, electrical stimulation, and real-time monitoring. Their integration combines biological fidelity with engineering precision, enabling high-throughput screening, dynamic evaluation, and optimization of therapeutic effects via embedded sensors [184]. Furthermore, coupling HoC systems with multi-organ chips may facilitate cross-organ functional and safety assessments, opening new avenues for myocardial regeneration, personalized therapy, and translational cardiovascular medicine [185]. Nevertheless, despite their advanced physiological relevance, these *in vitro* platforms cannot fully recapitulate the systemic complexity and long-term remodeling processes of myocardial infarction *in vivo*, thereby necessitating validation in animal models.

### 4.4 Achieving *in vivo* structural preservation and functional recovery in myocardial infarction models

In *in vivo* models of MI, force-electrical synergistic materials have demonstrated remarkable therapeutic potential. Their benefits encompass multiple dimensions, including promoting recovery of cardiac function, mitigating adverse structural remodeling and fibrosis, reconstructing electrical conduction networks, and improving the cardiac microenvironment [97].

Currently, most studies validate material efficacy using MI models generated by ligation of the left anterior descending coronary artery, with significant ST-segment elevation on electrocardiograms serving as the criterion for successful infarction induction [186]. At the functional level, force-electrical synergistic materials markedly improve LVEF and FS, while normalizing left ventricular diameters and volumes at end-systole and end-diastole, indicating substantial restoration of overall cardiac pumping function. For example, OGDPR hydrogels that possess both mechanical and electrical properties significantly enhance cardiac function *in vivo*. Echocardiographic measurements revealed increased LVEF and FS, along with improved left ventricular dimensions and volumes. At the same time, electrocardiography showed normalisation of Q waves and reduced ST-segment elevation, confirming effective functional recovery [187]. Moreover, conductive elastic cardiac patches fabricated via fused-embedded printing technology exhibited high conformity with native myocardium in terms of shape, mechanical compliance, and electrical conductivity. In MI models, these patches achieved excellent mechanical integration and significantly improved cardiac function, with LVEF increasing from 33.31% to 67.81%, underscoring the therapeutic efficacy of force-electrical synergy strategies in functional recovery [125]. At the tissue remodeling level, implantation of force-electrical synergistic materials reduce infarct size, alleviates collagen deposition, and increases ventricular wall thickness in the infarcted region. These effects are partly attributed to sustained mechanical support and stress distribution, which limit local stress concentration, reduce ventricular dilation, and inhibit fibrosis. Studies using microneedle-based engineered patches and conductive hydrogel patches with spatially regulated adhesion have demonstrated significant structural remodeling benefits, including reduced infarct size, decreased collagen deposition, and increased ventricular wall thickness [64, 188].

Further validation in rabbit MI models confirmed that these materials enhance ventricular wall support, limit dilation, and reduce fibrotic area, demonstrating stability of structural repair in higher-order animals [134].

Electrical integration is another critical therapeutic dimension. Force-electrical synergistic materials restore the expression and spatial distribution of the gap junction protein Cx43 in infarcted regions, enhance local conduction velocity, reduce ventricular arrhythmia incidence, and thus reconstruct myocardial force-electrical coupling. Conductive hydrogels containing reduced graphene oxide (rGO) upregulate Cx43 and cTnI expression by establishing continuous conductive networks, thereby enhancing conduction efficiency and synchronising electrical activity [154, 189, 190]. Similarly, conductive hook microneedle patches (CBMN-CP) improve Cx43 and *e*-actin expression and continuity within the infarct region, restoring effective myocardial electrical coupling by increasing interface stability and enlarging the conductive contact area [149]. Beyond mechanical and electrical support, force-electrical synergistic materials actively modulate the local microenvironment. For instance, OGDPR hydrogels reduce the expression of inflammatory factors and promote macrophage polarization from pro-inflammatory M1 to anti-inflammatory M2 phenotypes, thereby mitigating chronic inflammation and fibrosis [187, 191, 192]. Biodegradable, conductive, self-adhesive hydrogel patches further integrate electroactivity, mechanical matching, and wet adhesion to enhance vascular density and maturation, thereby demonstrating multidimensional therapeutic effects by promoting angiogenesis and regulating the microenvironment [126, 137, 193, 194]. Collectively, *in vivo* studies indicate that force-electrical synergistic platforms promote vascular reconstruction, reduce inflammation, attenuate collagen deposition and fibrosis, limit adverse ventricular remodeling, and restore coordinated cardiac function and electrical activity, highlighting their comprehensive therapeutic potential.

While demonstrating significant efficacy, *in vivo* degradation and biosafety remain critical for clinical translation. Most force-electrical synergistic materials are based on high-molecular-weight biodegradable matrices that degrade gradually via hydrolysis or enzymatic pathways and are absorbed over weeks to months [29, 195–197]. Histological and systemic hemolysis assessments indicate minimal inflammatory infiltration, no organ toxicity, and stable levels of inflammatory factors, confirming favorable acute and subacute biocompatibility [187, 198]. Immunomodulatory microneedle patches have also demonstrated excellent integration and biocompatibility in rodent and porcine MI models, with no chronic inflammation or organ toxicity, further supporting their translational potential [196]. Despite promising preclinical results, translating novel therapies into humans remains limited (~ 8% success over 40 years), highlighting the limitations of current models in predicting clinical outcomes [150, 199]. Challenges include large-scale material reproducibility, long-term maintenance of force-electrical properties under dynamic cardiac conditions, and potential chronic immune responses to conductive nanocomponents (e.g., rGO, metal nanoparticles, conductive polymers) [200]. Systematic elucidation of long-term biodistribution, metabolic pathways, and chronic toxicity is still required [200].

In parallel, humanized in vitro platforms such as cardiac organoids and organ-on-a-chip systems provide more physiologically relevant predictive tools for evaluating electrical integration and microenvironmental regulatory effects, complementing *in vivo* studies and informing material design [148, 200].

## 5 Conclusion and perspectives

Tissue damage of MI is characterized not only by extensive cardiomyocyte necrosis but also by the disruption of the heart's mechanical support structure and the imbalance of electrical signal conduction. In response to this complex pathological environment, biomaterials that modulate mechanical and electrical properties offer an innovative therapeutic strategy for restoring damaged myocardial function. This review summarizes recent advances in mechanical regulation, electrical modulation, and mechano-electrical coupling materials for MI repair, with an emphasis on the design principles and regulatory mechanisms that enable the reconstruction of the myocardial microenvironment and restoration of electrophysiological function through material property control. Furthermore, *in vitro* biomimetic models, such as cardiac organoids and HoC systems, offer powerful platforms for the systematic evaluation of electromechanical materials. These models not only facilitate performance screening and optimization of novel biomaterials but also, through the real-time monitoring capabilities of organ-on-a-chip technologies, enable precise regulation of material behavior under dynamic conditions. Looking ahead, the development of myocardial repair materials is expected to evolve toward greater intelligence and personalization. On the one hand, multimodal scaffolds incorporating neuroregulatory functions can be explored to co-reconstruct myocardial and neural networks by regulating neuronal signaling [8, 201]. On the other hand, dynamic material systems with spatiotemporal responsiveness can be engineered to adaptively adjust their mechanical, electrical, and biological properties across the different stages of myocardial repair, thereby guiding tissue regeneration with greater precision [132, 202, 203]. Meanwhile, successful clinical translation requires rigorous optimization of biocompatibility, biodegradability, immune safety, and compliance with regulatory standards to ensure safety and translational feasibility [177, 199, 204]. In conclusion, integrating mechano-electrical synergistic biomaterials with advanced biomimetic platforms not only provides novel strategies and insights for MI repair but also lays a solid foundation for the future development of intelligent and regenerative cardiovascular medicine.

## Data availability

Not applicable.

## Acknowledgements

This work was supported by the Strategic Priority Research Program of Chinese Academy of Sciences (No. XDA0580000), the National Natural Science Foundation of China (Nos. 22476031 and 22027810), the Directional Institutionalized Scientific Research Platform relies on the Beijing Synchrotron Radiation Facility of the Chinese Academy of Sciences (No. JZHKYPT-2021-02), and the State Key Laboratory of Biomacromolecules (No. 2025KF09).

## Declaration of competing interest

All the contributing authors report no conflict of interests in this work.

## Author contribution statement

M. K. Z. and J. M.: Data curation, validation, writing – original draft. Y. R., X. H., Z. B. C., M. X. J., C. B. L., Y. G. X., and Y. L. (Yi Liu): Data curation, validation. J. Y., C. Q. L., S. S. X., and Y. L. (Ying Liu): Project administration, writing – review & editing. Y. L. (Ying Liu): Project administration, funding acquisition. All the authors have approved the final manuscript.

## Informed consent

Not applicable.

## Ethics statement

Not applicable.

## Use of AI statement

None.

## References


[1] Thygesen, K.; Alpert, J. S.; Jaffe, A. S.; Chaitman, B. R.; Bax, J. J.; Morrow, D. A.; White, H. D.; Mickley, H.; Crea, F.; Van de Werf, F. et al. Fourth universal definition of myocardial infarction (2018). *Kardiol Pol* **2018**, *76*, 1383–1415.

[2] Sun, J. H.; Qiao, Y. N.; Zhao, M.; Magnussen, C. G.; Xi, B. Global, regional, and national burden of cardiovascular diseases in youths and young adults aged 15-39 years in 204 countries/territories, 1990-2019: A systematic analysis of global burden of disease study 2019. *BMC Med.* **2023**, *21*, 222.

[3] Chong, B.; Jayabaskaran, J.; Jauhari, S. M.; Chan, S. P.; Goh, R.; Kueh, M. T. W.; Li, H.; Chin, Y. H.; Kong, G.; Anand, V. V. et al. Global burden of cardiovascular diseases: Projections from 2025 to 2050. *Eur. J. Prev. Cardiol.* **2025**, *32*, 1001–1015.

[4] Rao, S. V.; O'Donoghue, M. L.; Ruel, M.; Rab, T.; Tamis-Holland, J. E.; Alexander, J. H.; Baber, U.; Baker, H.; Cohen, M. G.; Cruz-Ruiz, M. et al. 2025 ACC/AHA/ACEP/NAEMSP/SCAI guideline for the management of patients with acute coronary syndromes: A report of the American college of cardiology/American heart association joint committee on clinical practice guidelines. *J. Am. Coll. Cardiol.* **2025**, *85*, 2135–2237.

[5] Sagris, M.; Antonopoulos, A. S.; Theofilis, P.; Oikonomou, E.; Siasos, G.; Tsalamandris, S.; Antoniades, C.; Brilakis, E. S.; Kaski, J. C.; Tousoulis, D. Risk factors profile of young and older patients with myocardial infarction. *Cardiovasc. Res.* **2022**, *118*, 2281–2292.

[6] Christensen, D. M.; Schjerning, A. M.; Smedegaard, L.; Charlot, M. G.; Ravn, P. B.; Ruwald, A. C.; Fosbøl, E.; Køber, L.; Torp-Pedersen, C.; Schou, M. et al. Long-term mortality, cardiovascular events, and bleeding in stable patients 1 year after myocardial infarction: A Danish nationwide study. *Eur. Heart J.* **2023**, *44*, 488–498.

[7] Christensen, D. M.; El-Chouli, M.; Strange, J. E.; Nouhravesh, N.; Sindet-Pedersen, C.; Schjerning, A.; Schou, M.; Gislason, G.; Sehested, T. S. G. Long-term non-cardiovascular morbidity risk remains elevated following myocardial infarction: A nationwide cohort study. *Eur. Heart J.* **2022**, *43*, ehac544.1314.

[8] Zhou, W. X.; Rahman, M. S. U.; Sun, C. M.; Li, S. L.; Zhang, N. Z.; Chen, H.; Han, C. C.; Xu, S. S.; Liu, Y. Perspectives on the novel multifunctional nerve guidance conduits: From specific regenerative procedures to motor function rebuilding. *Adv. Mater.* **2024**, *36*, e2307805.

[9] Zhang, J. K.; Liu, C.; Li, J.; Yu, T.; Ruan, J.; Yang, F. Advanced piezoelectric materials, devices, and systems for orthopedic medicine. *Adv. Sci.* **2025**, *12*, e2410400.

[10] Wei, H.; Jing, H. C.; Cheng, C.; Liu, Y. Q.; Hao, J. C. A biomimetic one-stone-two-birds hydrogel with electroconductive, photothermally antibacterial and bioadhesive properties for skin tissue regeneration and mechanosensation restoration. *Adv. Funct. Mater.* **2025**, *35*, 2417280.

[11] Wei, Y. X.; Yu, Q. W.; Zhan, Y. X.; Wu, H.; Sun, Q. Piezoelectric hydrogels for accelerating healing of diverse wound types. *Biomater. Sci.* **2025**, *13*, 568–586.

[12] Zhang, Y. P.; Le Friec, A.; Zhang, Z. Y.; Müller, C. A.; Du, T. M.; Dong, M. D.; Liu, Y. J.; Chen, M. L. Electroactive biomaterials synergizing with electrostimulation for cardiac tissue regeneration and function-monitoring. *Mater. Today* **2023**, *70*, 237–272.

[13] Lv, Q. Q.; Zhou, D. D.; He, Y. T.; Xu, T.; Qiu, X. Z.; Zeng, J. W. Engineering functional electroconductive hydrogels for targeted therapy in myocardial infarction repair. *Bioact. Mater.* **2025**, *49*, 172–192.

[14] Wu, Y. B.; Wang, L.; Guo, B. L.; Ma, P. X. Interwoven aligned conductive nanofiber yarn/hydrogel composite scaffolds for engineered 3D cardiac anisotropy. *ACS Nano* **2017**, *11*, 5646–5659.

[15] Zhang, S. T.; Shao, Z. Y.; Wu, Y. H.; et al. The cardiac electrophysiology-inspired patches for repairing myocardial infarction: A review. *Smart Mater. Med.* **2025**, *6*, 108–119.

[16] Jia, X. M.; Liu, W. Y.; Ai, Y. J.; Cheung, S.; Hu, W. T.; Wang, Y.; Shi, X. L.; Zhou, J.; Zhang, Z.; Liang, Q. L. A multifunctional anisotropic patch manufactured by microfluidic manipulation for the repair of infarcted myocardium. *Adv. Mater.* **2024**, *36*, 2404071.

[17] Litviňuková, M.; Talavera-López, C.; Maatz, H.; Reichart, D.; Worth, C. L.; Lindberg, E. L.; Kanda, M.; Polanski, K.; Heinig, M.; Lee, M. et al. Cells of the adult human heart. *Nature* **2020**, *588*, 466–472.

[18] Trager, L. E.; Lyons, M.; Kuznetsov, A.; Sheffield, C.; Roh, K.; Freeman, R.; Rhee, J.; Guseh, J. S.; Li, H. B.; Rosenzweig, A. Beyond cardiomyocytes: Cellular diversity in the heart's response to exercise. *J. Sport Health Sci.* **2023**, *12*, 423–437.

[19] Quinn, T. A.; Kohl, P. Cardiac mechano-electric coupling: Acute effects of mechanical stimulation on heart rate and rhythm. *Physiol. Rev.* **2021**, *101*, 37–92.

[20] Izu, L. T.; Kohl, P.; Boyden, P. A.; Miura, M.; Banyasz, T.; Chiamvimonvat, N.; Trayanova, N.; Bers, D. M.; Chen-Izu, Y. Mechano-electric and mechano-chemo-transduction in cardiomyocytes. *J. Physiol.* **2020**, *598*, 1285–1305.

[21] Chen-Izu, Y.; Izu, L. T. Mechano-chemo-transduction in cardiac myocytes. *J. Physiol.* **2017**, *595*, 3949–3958.

[22] Bers, D. M. Cardiac excitation-contraction coupling. *Nature* **2002**, *415*, 198–205.

[23] Smith, C. E. R.; Grandi, E. Unveiling the intricacies of intracellular $Ca^{2+}$ regulation in the heart. *Biophys. J.* **2023**, *122*, 3019–3021.

[24] Seidler, T.; Hasenfuss, G.; Maier, L. S. Targeting altered calcium physiology in the heart: Translational approaches to excitation, contraction, and transcription. *Physiology* **2007**, *22*, 328–334.

[25] Guatimosim, S.; Dilly, K.; Santana, L. F.; Saleet Jafri, M.; Sobie, E. A.; Lederer, W. J. Local $Ca^{2+}$ signaling and EC coupling in heart: $Ca^{2+}$ sparks and the regulation of the $[Ca^{2+}]_i$ transient. *J. Mol. Cell Cardiol.* **2002**, *34*, 941–950.

[26] Chen-Izu, Y.; Banyasz, T.; Shaw, J. A.; Izu, L. T. The heart is a smart pump: Mechanotransduction mechanisms of the frank-starling law and the Anrep effect. *Annu. Rev. Physiol.* **2025**, *87*, 53–77.

[27] Ferrier, G. R.; Howlett, S. E. Cardiac excitation-contraction coupling: Role of membrane potential in regulation of contraction. *Am. J. Physiol. Heart Circ. Physiol.* **2001**, *280*, H1928–H1944.

[28] Mukherjee, A.; Huang, Y. Q.; Elgeti, J.; Oh, S.; Abreu, J. G.; Ammar, L.; Neliat, A. R.; Schüttler, J.; Su, D. D.; Dupre, C. et al. Membrane potential mediates the cellular response to mechanical pressure. *Cell* **2026**, *189*, 143–160.e22.

[29] Hume, R. D.; Kanagalingam, S.; Deshmukh, T.; Chen, S. Q.; Mithieux, S. M.; Rashid, F. N.; Roohani, I.; Lu, J. T.; Doan, T.; Graham, D. et al. Tropoelastin improves post-infarct cardiac function. *Circ. Res.* **2023**, *132*, 72–86.
[30] Chang, Z.; Zhang, J.; Liu, Y. L.; Gao, H. J.; Xu, G. K. New mechanical markers for tracking the progression of myocardial infarction. *Nano Lett.* **2023**, *23*, 7350–7357.
[31] Li, S. M.; Yin, W. M.; Liu, Y. L.; Yang, C.; Zhai, Z. T.; Xie, M. X.; Ye, Z. Y.; Song, X. P. Anisotropic conductive scaffolds for post-infarction cardiac repair. *Biomater. Sci.* **2025**, *13*, 542–567.
[32] Berry, M. F.; Engler, A. J.; Woo, Y. J.; Pirolli, T. J.; Bish, L. T.; Jayasankar, V.; Morine, K. J.; Gardner, T. J.; Discher, D. E.; Sweeney, H. L. Mesenchymal stem cell injection after myocardial infarction improves myocardial compliance. *Am. J. Physiol. Heart Circ. Physiol.* **2006**, *290*, H2196–H2203.
[33] Wang, Z. J.; Santiago, A.; Zhou, X.; Wang, L.; Margara, F.; Levrero-Florencio, F.; Das, A.; Kelly, C.; Dall'Armellina, E.; Vazquez, M. et al. Human biventricular electromechanical simulations on the progression of electrocardiographic and mechanical abnormalities in post-myocardial infarction. *EP Eur.* **2021**, *23*, i143–i152.
[34] Niu, H.; Liu, Z. T.; Guan, Y.; Wen, J. X.; Dang, Y.; Guan, J. J. Harnessing synergistic effects of MMP-2 Inhibition and bFGF to simultaneously preserve and vascularize cardiac extracellular matrix after myocardial infarction. *Acta Biomater.* **2025**, *191*, 189–204.
[35] Sullivan, K. E.; Quinn, K. P.; Tang, K. M.; Georgakoudi, I.; Black III, L. D. Extracellular matrix remodeling following myocardial infarction influences the therapeutic potential of mesenchymal stem cells. *Stem Cell Res. Ther.* **2014**, *5*, 14.
[36] Dwyer, K. D.; Coulombe, K. L. K. Cardiac mechanostructure: Using mechanics and anisotropy as inspiration for developing epicardial therapies in treating myocardial infarction. *Bioact. Mater.* **2021**, *6*, 2198–2220.
[37] Fadle Aziz, M. R.; Wlodarek, L.; Alibhai, F.; Wu, J.; Li, S. H.; Sun, Y.; Santerre, J. P.; Li, R. K. A polypyrrole-polycarbonate polyurethane elastomer alleviates cardiac arrhythmias via improving bio-conductivity. *Adv. Healthc. Mater.* **2023**, *12*, e2203168.
[38] Yang, F.; Zhang, X. L.; Liu, H. H.; Qian, L. L.; Wang, R. X. Post translational modifications of connexin 43 in ventricular arrhythmias after myocardial infarction. *Mol. Biol. Rep.* **2024**, *51*, 329.
[39] Beardslee, M. A.; Lerner, D. L.; Tadros, P. N.; Laing, J. G.; Beyer, E. C.; Yamada, K. A.; Kleber, A. G.; Schuessler, R. B.; Saffitz, J. E. Dephosphorylation and intracellular redistribution of ventricular connexin43 during electrical uncoupling induced by ischemia. *Circ. Res.* **2000**, *87*, 656–662.
[40] Jie, X.; Gurev, V.; Trayanova, N. Mechanisms of mechanically induced spontaneous arrhythmias in acute regional ischemia. *Circ. Res.* **2010**, *106*, 185–192.
[41] Mørk, H. K.; Sjaastad, I.; Sejersted, O. M.; Louch, W. E. Slowing of cardiomyocyte $Ca^{2+}$ release and contraction during heart failure progression in postinfarction mice. *Am. J. Physiol. Heart Circ. Physiol.* **2009**, *296*, H1069–H1079.
[42] Wasserstrom, J. A.; Holt, E.; Sjaastad, I.; Lunde, P. K.; Ødegaard, A.; Sejersted, O. M. Altered E-C coupling in rat ventricular myocytes from failing hearts 6 wk after MI. *Am. J. Physiol. Heart Circ. Physiol.* **2000**, *279*, H798–H807.
[43] Kim, I. G.; Hwang, M. P.; Park, J. S.; Kim, S. H.; Kim, J. H.; Kang, H. J.; Subbiah, R.; Ko, U. H.; Shin, J. H.; Kim, C. H. et al. Stretchable ECM patch enhances stem cell delivery for post-MI cardiovascular repair. *Adv. Healthc. Mater.* **2019**, *8*, 1900593.
[44] Li, Y. R.; Du, J. L.; Deng, S. B.; Liu, B.; Jing, X. D.; Yan, Y. L.; Liu, Y. J.; Wang, J.; Zhou, X. B.; She, Q. The molecular mechanisms of cardiac development and related diseases. *Signal Transduct. Target. Ther.* **2024**, *9*, 368.
[45] Domian, I. J.; Yu, H.; Mittal, N. On materials for cardiac tissue engineering. *Adv. Healthc. Mater.* **2017**, *6*, 1600768.
[46] Baghersad, S.; Sathish Kumar, A.; Kipper, M. J.; Popat, K.; Wang, Z. J. Recent advances in tissue-engineered cardiac scaffolds-the progress and gap in mimicking native myocardium mechanical behaviors. *J. Funct. Biomater.* **2023**, *14*, 269.
[47] Meyers, K.; Lee, B. P.; Rajachar, R. M. Electroactive polymeric composites to mimic the electromechanical properties of myocardium in cardiac tissue repair. *Gels* **2021**, *7*, 53.
[48] Yu, C. J.; Qiu, Y. W.; Yao, F. L.; Wang, C. Y.; Li, J. J. Chemically programmed hydrogels for spatiotemporal modulation of the cardiac pathological microenvironment. *Adv. Mater.* **2024**, *36*, 2404264.
[49] Fischer, A. G.; Elliott, E. M.; Brittian, K. R.; Garrett, L.; Sadri, G.; Aebersold, J.; Singhal, R. A.; Nong, Y. B.; Leask, A.; Jones, S. P. et al. Matricellular protein CCN1 promotes collagen alignment and scar integrity after myocardial infarction. *Matrix Biol.* **2024**, *133*, 14–32.
[50] Yap, J.; Irei, J.; Lozano-Gerona, J.; Vanapruks, S.; Bishop, T.; Boisvert, W. A. Macrophages in cardiac remodelling after myocardial infarction. *Nat. Rev. Cardiol.* **2023**, *20*, 373–385.
[51] Murphy, S. P.; Ibrahim, N. E.; Januzzi, J. L. Jr. Heart failure with reduced ejection fraction: A review. *JAMA* **2020**, *324*, 488–504.
[52] Whittaker, P. Collagen and ventricular remodeling after acute myocardial infarction: Concepts and hypotheses. *Basic Res. Cardiol.* **1997**, *92*, 79–81.
[53] Yu, D. M.; Wang, X. W.; Ye, L. Cardiac tissue engineering for the treatment of myocardial infarction. *J. Cardiovasc. Dev. Dis.* **2021**, *8*, 153.
[54] Naahidi, S.; Jafari, M.; Logan, M.; Wang, Y. J.; Yuan, Y. F.; Bae, H.; Dixon, B.; Chen, P. Biocompatibility of hydrogel-based scaffolds for tissue engineering applications. *Biotechnol. Adv.* **2017**, *35*, 530–544.
[55] Wang, C. H.; Liu, Z. F.; Zhang, N. Z.; Huang, S. F.; Mao, R. Q.; Wang, H. R.; Xia, Q. H.; Han, C. C.; Xu, S. S.; Liu, Y. Three dimensional fibrous scaffolds as tissue repairing templates during post-operative healing. *Mater. Des.* **2021**, *210*, 110019.
[56] Liu, W.; Zhang, X. M.; Jiang, X. K.; Dai, B. Y.; Zhang, L. W.; Zhu, Y. Decellularized extracellular matrix materials for treatment of ischemic cardiomyopathy. *Bioact. Mater.* **2024**, *33*, 460–482.
[57] Tian, J. K.; Yang, H. L.; Chang, L. L.; Zhang, X.; Wang, W. T.; Li, R. W. Hydrogel based scaffolds in cardiovascular disease: Applications in myocardial regeneration, biological pacing, and heart failure therapy. *Front. Cell Dev. Biol.* **2025**, *13*, 1678848.
[58] Majid, Q. A.; Fricker, A. T. R.; Gregory, D. A.; Davidenko, N.; Hernandez Cruz, O.; Jabbour, R. J.; Owen, T. J.; Basnett, P.; Lukasiewicz, B.; Stevens, M. et al. Natural biomaterials for cardiac tissue engineering: A highly biocompatible solution. *Front. Cardiovasc. Med.* **2020**, *7*, 554597.
[59] Efraim, Y.; Sarig, H.; Cohen Anavy, N.; Sarig, U.; de Berardinis, E.; Chaw, S. Y.; Krishnamoorthi, M.; Kalifa, J.; Bogireddi, H.; Duc, T. V. et al. Biohybrid cardiac ECM-based hydrogels improve long term cardiac function post myocardial infarction. *Acta Biomater.* **2017**, *50*, 220–233.
[60] Li, Z. T.; Li, Q.; Cao, W. D.; Zhan, J. M.; He, Y. T.; Xing, X. L.; Ding, C. B.; Wang, L. Y.; Qiu, X. Z. A strongly robust chitosan-based programmed control functional hydrogel improved mitochondrial function and pro-vascularization for adaptive repair of myocardial infarction. *Adv. Funct. Mater.* **2024**, *34*, 2312631.
[61] Shan, M. Q.; Wei, L. Q.; Yang, Z. Q.; Li, Y. M.; Deng, R. L.; Zhao, X. Z.; Wang, F. J.; Wang, G. X.; Wang, L.; Mao, J. F. An anisotropic cardiac patch with barbed microneedles for enhanced tissue anchorage and myocardial repair. *Acta Biomater.* **2025**, *205*, 505–520.
[62] Liang, Q. H.; Chen, S. H.; Hua, S. F.; Jiang, W. H.; Zhan, J. M.; Pu, C. Y.; Lin, R. R.; He, Y. T.; Hou, H. H.; Qiu, X. Z. Biomimetic versatile anisotropic, electroactive cellulose hydrogel scaffolds tailored from fern stem serving as nerve conduit and cardiac patch. *Adv. Sci.* **2025**, *12*, 2400002.
[63] Lv, Y. C.; Zhou, X. Y.; Wang, M. Y.; Qi, M. Y.; Xie, W. Q.; Liu, C.; Dong, Z. X.; Fu, X. L. Mitochondria-loaded Janus cardiac patch for

myocardial infarction repair and prevention of tissue adhesions. *ACS Nano* **2026**, *20*, 1462–1480.

[64] Zhang, Y. X.; Xu, Y. Y.; Wu, C.; Chen, S. Y.; Chen, Z. Y.; Qin, F.; Hu, X. F.; Zhang, J. Y.; Wang, Y. B. Injectable conductive hydrogel patch with spatiotemporally tailored asymmetric adhesion for myocardial infarction repair. *Adv. Mater.* **2026**, *38*, e10824.

[65] Qiu, Y. L.; Bayomy, A. F.; Gomez, M. V.; Bauer, M.; Du, P.; Yang, Y. F.; Zhang, X.; Liao, R. A role for matrix stiffness in the regulation of cardiac side population cell function. *Am. J. Physiol. Heart Circ. Physiol.* **2015**, *308*, H990–H997.

[66] Moazzam, M. Dual-crosslinked hydrogels for tissue engineering: A comprehensive systematic review and meta-analysis of emerging strategies. *CAR*, in press, DOI: 10.36922/CAR025400001.

[67] Wang, Y. T.; Meng, D. N.; Shi, X. H.; Hou, Y.; Zang, S. H.; Chen, L.; Spanos, M.; Li, G. P.; Cretoiu, D.; Zhou, Q. L. et al. Injectable hydrogel with miR-222-engineered extracellular vesicles ameliorates myocardial ischemic reperfusion injury via mechanotransduction. *Cell Rep. Med.* **2025**, *6*, 101987.

[68] Ghanbari, E.; Solouk, A.; Mehdinavaz Aghdam, R.; Haghbin Nazarpak, M.; Ahmadi Tafti, S. H. A novel substrate based on electrospun polyurethane nanofibers and electrosprayed polyvinyl alcohol microparticles for recombinant human erythropoietin delivery. *J. Biomed. Mater. Res. A* **2022**, *110*, 181–195.

[69] Yang, Y.; Lei, D.; Huang, S. X.; Yang, Q.; Song, B. Y.; Guo, Y. F.; Shen, A.; Yuan, Z. Z.; Li, S.; Qing, F. L. et al. Elastic 3D-printed hybrid polymeric scaffold improves cardiac remodeling after myocardial infarction. *Adv. Healthc. Mater.* **2019**, *8*, 1900065.

[70] Chemla, D.; Coirault, C.; Hébert, J. L.; Lecarpentier, Y. Mechanics of relaxation of the human heart. *News Physiol. Sci.* **2000**, *15*, 78–83.

[71] Fu, L. Y.; Han, K.; Qi, J.; Lei, Q.; Wang, X. M.; Wu, J. M.; Yang, N.; Li, Y.; Kang, Y. M.; Yu, X. J. et al. Electrohydrodynamically-printed serpentine fiber scaffolds with enhanced conductivity and elasticity for post-myocardial infarction repair. *Acta Biomater.* **2025**, *200*, 476–488.

[72] Wang, Y. W.; Fan, Z. P.; Li, Q.; Lu, J. L.; Wang, X. Y.; Zhang, J. H.; Wu, Z. Construction of a myocardial patch with mesenchymal stem cells and poly(CL-*co*-TOSUO)/collagen scaffolds for myocardial infarction repair by coaxial electrospinning. *J. Mater. Chem. B* **2023**, *11*, 4980–4990.

[73] Chen, T. A.; Zhao, B. B.; Balbin, R. A.; Sharma, S.; Ha, D.; Kamp, T. J.; Zhou, Y. X.; Zhao, F. Engineering a robust and anisotropic cardiac-specific extracellular matrix scaffold for cardiac patch tissue engineering. *Matrix Biol. Plus* **2024**, *23*, 100151.

[74] Davidenko, N.; Schuster, C. F.; Bax, D. V.; Raynal, N.; Farndale, R. W.; Best, S. M.; Cameron, R. E. Control of crosslinking for tailoring collagen-based scaffolds stability and mechanics. *Acta Biomater.* **2015**, *25*, 131–142.

[75] Xu, C. C.; Okpokwasili, C.; Huang, Y. H.; Shi, X. D.; Wu, J. L.; Liao, J.; Tang, L. P.; Hong, Y. Optimizing anisotropic polyurethane scaffolds to mechanically match with native myocardium. *ACS Biomater. Sci. Eng.* **2020**, *6*, 2757–2769.

[76] Cui, H. T.; Yu, Z. X.; Huang, Y. M.; Hann, S. Y.; Esworthy, T.; Shen, Y. L.; Zhang, L. G. 3D printing of thick myocardial tissue constructs with anisotropic myofibers and perfusable vascular channels. *Biomater. Adv.* **2023**, *153*, 213579.

[77] Ahrens, J. H.; Uzel, S. G. M.; Skylar-Scott, M.; Mata, M. M.; Lu, A.; Kroll, K. T.; Lewis, J. A. Programming cellular alignment in engineered cardiac tissue via bioprinting anisotropic organ building blocks. *Adv. Mater.* **2022**, *34*, 2200217.

[78] Cyr, J. A.; Burdett, C.; Pürstl, J. T.; Thompson, R. P.; Troughton, S. C.; Sinha, S.; Best, S. M.; Cameron, R. E. Characterizing collagen scaffold compliance with native myocardial strains using an *ex-vivo* cardiac model: The physio-mechanical influence of scaffold architecture and attachment method. *Acta Biomater.* **2024**, *184*, 239–253.

[79] Montgomery, M.; Ahadian, S.; Davenport Huyer, L.; Lo Rito, M.; Civitarese, R. A.; Vanderlaan, R. D.; Wu, J.; Reis, L. A.; Momen, A.; Akbari, S. et al. Flexible shape-memory scaffold for minimally invasive delivery of functional tissues. *Nat. Mater.* **2017**, *16*, 1038–1046.

[80] Xu, S. S.; Wang, C. H.; Mao, R. Q.; Liang, X. Y.; Wang, H. R.; Lin, Z. Y.; Li, J. X.; Li, S. L.; Jiang, J. P.; Zhang, T. S. et al. Surface structure change properties: Auto-soft bionic fibrous membrane in reducing postoperative adhesion. *Bioact. Mater.* **2022**, *12*, 16–29.

[81] Sun, D.; Wang, H.; Liu, J.; Wang, X. L.; Guo, H. B.; Xue, L. J.; Li, L. B.; Li, J. B.; Zhang, B. J.; Xue, Y. G. et al. An enzyme cross-linked hydrogel as a minimally invasive arterial tissue sealing and anti-adhesion barrier. *Nano Today* **2022**, *44*, 101467.

[82] Lu, Y. W.; Ren, T. C.; Zhang, H.; Jin, Q.; Shen, L. Y.; Shan, M. Q.; Zhao, X. Z.; Chen, Q. C.; Dai, H. L.; Yao, L. et al. A honeybee stinger-inspired self-interlocking microneedle patch and its application in myocardial infarction treatment. *Acta Biomater.* **2022**, *153*, 386–398.

[83] Gan, D. L.; Xing, W. S.; Jiang, L. L.; Fang, J.; Zhao, C. C.; Ren, F. Z.; Fang, L. M.; Wang, K. F.; Lu, X. Plant-inspired adhesive and tough hydrogel based on Ag-Lignin nanoparticles-triggered dynamic redox catechol chemistry. *Nat. Commun.* **2019**, *10*, 1487.

[84] Chen, S. L.; Liu, J.; Li, D. P.; Wen, Y.; Huang, Y. W.; Long, S. J.; Li, X. F. An all-natural polymer-based and bilayer-integrated asymmetrical Janus hydrogel bioadhesive patch for cardiac repair. *Biomacromolecules* **2025**, *26*, 4248–4261.

[85] He, Y. T.; Li, Q.; Chen, P. F.; Duan, Q. X.; Zhan, J. M.; Cai, X. H.; Wang, L. Y.; Hou, H. H.; Qiu, X. Z. A smart adhesive Janus hydrogel for non-invasive cardiac repair and tissue adhesion prevention. *Nat. Commun.* **2022**, *13*, 7666.

[86] Chen, S.; Tan, L. D.; Serpooshan, V.; Chen, H. F. A 3D bioprinted adhesive tissue engineering scaffold to repair ischemic heart injury. *Biomater. Sci.* **2025**, *13*, 506–522.

[87] Zhang, Q.; Yang, Y. H.; Suo, D.; Zhao, S.; Cheung, J. C. W.; Leung, P. H. M.; Zhao, X. A biomimetic adhesive and robust janus patch with anti-oxidative, anti-inflammatory, and anti-bacterial activities for tendon repair. *ACS Nano* **2023**, *17*, 16798–16816.

[88] Liao, Y. J.; He, L.; Zhang, Z. S.; Geng, S. H.; Ren, Q. L. Advanced conductive biomaterials for cardiac tissue: Design and engineering applications. *Chem. Eng. J.* **2025**, *525*, 170294.

[89] Li, Y. M.; Wei, L. Q.; Lan, L. Z.; Gao, Y. Y.; Zhang, Q.; Dawit, H.; Mao, J. F.; Guo, L. M.; Shen, L.; Wang, L. Conductive biomaterials for cardiac repair: A review. *Acta Biomater.* **2022**, *139*, 157–178.

[90] Aboagye, J.; Edwards, M.; Ge, J.; Hong, Y.; Yang, H. X. Evaluating and improving biocompatibility of conductive polymers for cardiac tissue engineering. *J. Mater. Chem. B* **2026**, *14*, 775–798.

[91] Razavi, Z. S.; Farokhi, S.; Mahmoudvand, G.; Karimi-Rouzbahani, A.; Farasati-Far, B.; Tahmasebi-Ghorabi, S.; Pazoki-Toroudi, H.; Saadat-Fakhr, M.; Afkhami, H. Stem cells and bio scaffolds for the treatment of cardiovascular diseases: New insights. *Front. Cell Dev. Biol.* **2024**, *12*, 1472103.

[92] Liu, Y.; Zhao, Y. L.; Sun, B. Y.; Chen, C. Y. Understanding the toxicity of carbon nanotubes. *Acc. Chem. Res.* **2013**, *46*, 702–713.

[93] Lee, M.; Park, J.; Choe, G.; Lee, S.; Kang, B. G.; Jun, J. H.; Shin, Y.; Kim, M. C.; Kim, Y. S.; Ahn, Y. et al. A conductive and adhesive hydrogel composed of MXene nanoflakes as a paintable cardiac patch for infarcted heart repair. *ACS Nano* **2023**, *17*, 12290–12304.

[94] Alamdari, S. G.; Alibakhshi, A.; de la Guardia, M.; Baradaran, B.; Mohammadzadeh, R.; Amini, M.; Kesharwani, P.; Mokhtarzadeh, A.; Oroojalian, F.; Sahebkar, A. Conductive and semiconductive nanocomposite-based hydrogels for cardiac tissue engineering. *Adv. Healthc. Mater.* **2022**, *11*, 2200526.

[95] Li, H. K.; Yu, B.; Yang, P. Z.; Zhan, J.; Fan, X. L.; Chen, P. E.; Liao, X.; Ou, C. W.; Cai, Y. B.; Chen, M. S. Injectable AuNP-HA matrix with localized stiffness enhances the formation of gap junction in engrafted human induced pluripotent stem cell-derived

cardiomyocytes and promotes cardiac repair. *Biomaterials* **2021**, *279*, 121231.

[96] Choi, S.; Lee, K. Y.; Kim, S. L.; MacQueen, L. A.; Chang, H. B.; Zimmerman, J. F.; Jin, Q. R.; Peters, M. M.; Ardoña, H. A. M.; Liu, X. J. et al. Fibre-infused gel scaffolds guide cardiomyocyte alignment in 3D-printed ventricles. *Nat. Mater.* **2023**, *22*, 1039–1046.

[97] Liu, T. L.; Hao, Y.; Zhang, Z. X.; Zhou, H.; Peng, S. Q.; Zhang, D. Y.; Li, K.; Chen, Y. W.; Chen, M. Advanced cardiac patches for the treatment of myocardial infarction. *Circulation* **2024**, *149*, 2002–2020.

[98] Bai, L.; Luo, Q. H.; Gao, Z. S.; Wang, Y.; Wu, Y.; Yuan, D. C.; Liu, M. D.; Hu, C.; Wang, Y. B. Bioinspired conductive structural color hydrogels: A theragnostic platform for spatiotemporal monitoring and repair of myocardial infarction. *Adv. Funct. Mater.* **2025**, *35*, 10548.

[99] Liu, Y.; Chen, C. Y.; Qian, P. X.; Lu, X. F.; Sun, B. Y.; Zhang, X.; Wang, L. M.; Gao, X. F.; Li, H.; Chen, Z. Y. et al. Gd-metallofullerenol nanomaterial as non-toxic breast cancer stem cell-specific inhibitor. *Nat. Commun.* **2015**, *6*, 5988.

[100] Yin, Q.; Zhu, P.; Liu, W.; Gao, Z. B.; Zhao, L. M.; Wang, C. L.; Li, S. W.; Zhu, M. M.; Zhang, Q.; Zhang, X. et al. A conductive bioengineered cardiac patch for myocardial infarction treatment by improving tissue electrical integrity. *Adv. Healthc. Mater.* **2023**, *12*, 2201856.

[101] Zhang, L. H.; Li, T.; Yu, Y.; Shi, K.; Bei, Z. W.; Qian, Y. J.; Qian, Z. Y. An injectable conductive hydrogel restores electrical transmission at myocardial infarct site to preserve cardiac function and enhance repair. *Bioact. Mater.* **2023**, *20*, 339–354.

[102] Yu, S.; Wang, L.; Chen, M. D.; Chen, Y. J.; Peng, Z. B. MXene-incorporated conductive hydrogel simulating myocardial microenvironment for cardiac repair and functional recovery. *Biomacromolecules* **2025**, *26*, 2378–2389.

[103] Xu, Z. Y.; Hong, W. Z.; Mo, Y. X.; Shu, F.; Liu, Y. X.; Cheng, Y. Q.; Tan, N.; Jiang, L. Stem cells derived exosome laden oxygen generating hydrogel composites with good electrical conductivity for the tissue-repairing process of post-myocardial infarction. *J. Nanobiotechnol.* **2025**, *23*, 213.

[104] Chen, X. R.; Chen, H.; Zhu, L. Y.; Zeng, M. T.; Wang, T. H.; Su, C. Y.; Vulugundam, G.; Gokulnath, P.; Li, G. P.; Wang, X. et al. Nanoparticle-patch system for localized, effective, and sustained miRNA administration into infarcted myocardium to alleviate myocardial ischemia-reperfusion injury. *ACS Nano* **2024**, *18*, 19470–19488.

[105] Wang, M. J.; Li, S. L.; Chen, Z. J.; Zhu, J. B.; Hao, W. D.; Jia, G.; Chen, W.; Zheng, Y. X.; Qu, W. D.; Liu, Y. Safety assessment of nanoparticles in food: Current status and prospective. *Nano Today* **2021**, *39*, 101169.

[106] Greiner, J.; Sankarankutty, A. C.; Seidel, T.; Sachse, F. B. Confocal microscopy-based estimation of intracellular conductivities in myocardium for modeling of the normal and infarcted heart. *Comput. Biol. Med.* **2022**, *146*, 105579.

[107] Li, X.; Ren, Y.; Xue, Y. G.; Zhang, Y. M.; Liu, Y. Nanofibrous scaffolds for the healing of the fibrocartilaginous enthesis: Advances and prospects. *Nanoscale Horiz.* **2023**, *8*, 1313–1332.

[108] Qi, H. N.; Jing, X. L.; Hu, Y. L.; Wu, P.; Zhang, X. J.; Li, Y. T.; Zhao, H. K.; Ma, Q. L.; Dong, X. T.; Mahadevan, C. K. Electrospun green fluorescent-highly anisotropic conductive Janus-type nanoribbon hydrogel array film for multiple stimulus response sensors. *Compos. Part B: Eng.* **2025**, *288*, 111933.

[109] Zhang, C. W.; Si, M. Q.; Chen, C.; He, P.; Fei, Z. Q.; Xu, N.; He, X. M. Hierarchical engineering for biopolymer-based hydrogels with tailored property and functionality. *Adv. Mater.* **2025**, *37*, 2414897.

[110] Li, N.; Yu, Q. Y.; Duan, S. D.; Du, Y. J.; Shi, X. J.; Li, X. Y.; Jiao, T. F.; Qin, Z. H.; He, X. M. Anti-swelling, high-strength, anisotropic conductive hydrogel with excellent biocompatibility for implantable electronic tendon. *Adv. Funct. Mater.* **2024**, *34*, 2309500.

[111] Liu, Z. F.; Wang, L.; Ren, Y.; Chen, H.; Li, S. J.; Li, S. L.; Xu, S. S.; Liu, Y. Protective effectiveness of electrospinning fibrous membrane in inguinal hernia repair. *Mater. Des.* **2023**, *231*, 112074.

[112] Wang, J. M.; Liu, Q.; Gong, J. X.; Wan, Z. J.; Zhou, J. P.; Chang, C. Y.; Zhang, D. H. Micropatterned hydrogels with highly ordered cellulose nanocrystals for visually monitoring cardiomyocytes. *Small* **2022**, *18*, 2202235.

[113] Zhao, G. X.; Feng, Y. J.; Xue, L.; Cui, M. J.; Zhang, Q.; Xu, F.; Peng, N. C.; Jiang, Z. D.; Gao, D. F.; Zhang, X. H. Anisotropic conductive reduced graphene oxide/silk matrices promote post-infarction myocardial function by restoring electrical integrity. *Acta Biomater.* **2022**, *139*, 190–203.

[114] Basara, G.; Saeidi-Javash, M.; Ren, X.; Bahcecioglu, G.; Wyatt, B. C.; Anasori, B.; Zhang, Y. L.; Zorlutuna, P. Electrically conductive 3D printed $Ti_3C_2T_x$ MXene-PEG composite constructs for cardiac tissue engineering. *Acta Biomater.* **2022**, *139*, 179–189.

[115] Zhang, G. H.; Chen, Y. D.; Zhou, W. X.; Chen, C. Y.; Liu, Y. Bioenergy-based closed-loop medical systems for the integration of treatment, monitoring, and feedback. *Small Sci.* **2023**, *3*, 2300043.

[116] Tamo, A. K.; Doench, I.; Roshanbinfar, K.; Montembault, A.; Serghei, A.; Engel, F. B.; Osorio-Madrazo, A. Electrically conductive biopolymer-based hydrogels and fibrous materials fabricated using 3D printing and electrospinning for cardiac tissue engineering. *Bioact. Mater.* **2025**, *51*, 650–719.

[117] Li, M. Y.; Guo, Y.; Wei, Y.; MacDiarmid, A. G.; Lelkes, P. I. Electrospinning polyaniline-contained gelatin nanofibers for tissue engineering applications. *Biomaterials* **2006**, *27*, 2705–2715.

[118] Sapir, Y.; Kryukov, O.; Cohen, S. Integration of multiple cell-matrix interactions into alginate scaffolds for promoting cardiac tissue regeneration. *Biomaterials* **2011**, *32*, 1838–1847.

[119] Qazi, T. H.; Rai, R.; Dippold, D.; Roether, J. E.; Schubert, D. W.; Rosellini, E.; Barbani, N.; Boccaccini, A. R. Development and characterization of novel electrically conductive PANI-PGS composites for cardiac tissue engineering applications. *Acta Biomater.* **2014**, *10*, 2434–2445.

[120] Jalilinejad, N.; Rabiee, M.; Baheiraei, N.; Ghahremanzadeh, R.; Salarian, R.; Rabiee, N.; Akhavan, O.; Zarrintaj, P.; Hejna, A.; Saeb, M. R. et al. Electrically conductive carbon-based (bio)-nanomaterials for cardiac tissue engineering. *Bioeng. Transl. Med.* **2022**, *8*, e10347.

[121] Lee, J.; Manoharan, V.; Cheung, L.; Lee, S.; Cha, B. H.; Newman, P.; Farzad, R.; Mehrotra, S.; Zhang, K. Z.; Khan, F. et al. Nanoparticle-based hybrid scaffolds for deciphering the role of multimodal cues in cardiac tissue engineering. *ACS Nano* **2019**, *13*, 12525–12539.

[122] Zhang, Y.; Mu, W. Y.; Zhang, Y. P.; He, X. T.; Wang, Y. M.; Ma, H. Y.; Zhu, T. Y.; Li, A. Y.; Hou, Q. Z.; Yang, W. M. et al. Recent advances in cardiac patches: Materials, preparations, and properties. *ACS Biomater. Sci. Eng.* **2022**, *8*, 3659–3675.

[123] Leung, M. C.; Laksman, Z. 3D bioprinting functional engineered heart tissues. *Int. J. Mol. Sci.* **2025**, *26*, 10707.

[124] Wang, Z. H.; Wang, L.; Li, T.; Liu, S. T.; Guo, B. L.; Huang, W. H.; Wu, Y. B. 3D bioprinting in cardiac tissue engineering. *Theranostics* **2021**, *11*, 7948–7969.

[125] Zeng, X. B.; Li, Z. L.; Tan, X.; Ren, Z. S.; Gao, J. Y.; Meng, Z. J.; Li, D. C.; Fan, J. H.; Mao, M.; Guo, B. L. et al. Melt-based embedded printing of macroscopically-conformal, electro-conductive and elastomeric patches for improved myocardial infarction repair. *Adv. Mater.* **2026**, *38*, e12137.

[126] Zheng, Z.; Lei, C.; Liu, H. B.; Jiang, M. C.; Zhou, Z. T.; Zhao, Y. Q.; Yu, C. Y.; Wei, H. A ROS-responsive liposomal composite hydrogel integrating improved mitochondrial function and pro-angiogenesis for efficient treatment of myocardial infarction. *Adv. Healthc. Mater.* **2022**, *11*, 2200990.

[127] Lu, J. J.; Chen, J.; Lu, L. K.; Zhao, Y. T.; Liu, R. Q.; Li, Y. R.; Liu, C. G.; Che, P. C.; Sun, H. An injectable multifunctional hydrogel for cardiac spatiotemporal repair via modulating oxidative stress and the inflammatory microenvironment. *J. Mater. Chem. B* **2026**, *14*, 248–260.

[128] Jia, M. X.; Wang, J. M.; Lin, C. B.; Zhang, Q. Y.; Xue, Y. G.; Huang, X.; Ren, Y.; Chen, C. Y.; Liu, Y.; Xu, Y. W. Hydrogel strategies for female reproduction dysfunction. *ACS Nano* **2024**, *18*, 30132–30152.

[129] Ren, Y.; Yuan, J.; Xue, Y. G.; Zhang, Y. M.; Li, S. L.; Liu, C. Q.; Liu, Y. Advanced hydrogels: New expectation for the repair of organic erectile dysfunction. *Mater. Today Bio* **2023**, *19*, 100588.

[130] Yu, C. J.; Yue, Z. W.; Shi, M. Y.; Jiang, L. J.; Chen, S.; Yao, M. M.; Yu, Q. Y.; Wu, X. J.; Zhang, H.; Yao, F. L. et al. An intrapericardial injectable hydrogel patch for mechanical-electrical coupling with infarcted myocardium. *ACS Nano* **2022**, *16*, 16234–16248.

[131] Kapnisi, M.; Mansfield, C.; Marijon, C.; Guex, A. G.; Perbellini, F.; Bardi, I.; Humphrey, E. J.; Puetzer, J. L.; Mawad, D.; Koutsogeorgis, D. C. et al. Auxetic cardiac patches with tunable mechanical and conductive properties toward treating myocardial infarction. *Adv. Funct. Mater.* **2018**, *28*, 1800618.

[132] Qiu, Y. W.; Yu, C. J.; Yue, Z. W.; Ren, Y. C.; Wang, W. T.; Yu, Q. Y.; Guo, B. Y.; Liang, L.; Yao, F. L.; Zhang, H. et al. Chronological-programmed black phosphorus hydrogel for responsive modulation of the pathological microenvironment in myocardial infarction. *ACS Appl. Mater. Interfaces* **2024**, *16*, 17323–17338.

[133] Guo, M. Y.; Bi, S. Y.; Liu, J.; Xu, W. S.; Zhou, G. Q.; Liu, Y.; Chen, C. Y. $C_{60}(OH)_n$-loaded nanofibrous membranes protect HaCaT cells from ROS-associated damage. *Chin. Chem. Lett.* **2017**, *28*, 1889–1892.

[134] Zhang, F.; Zhang, Y. K.; Qian, S. C.; Qian, X. T.; Jiao, J. C.; Ma, B.; Chen, J. Z.; Cheng, H. Y.; Li, X. P.; Lin, Y. P. et al. Injectable and conductive nanomicelle hydrogel with α-tocopherol encapsulation for enhanced myocardial infarction repair. *ACS Nano* **2024**, *18*, 10216–10229.

[135] Karimi Hajishoreh, N.; Baheiraei, N.; Naderi, N.; Salehnia, M.; Razavi, M. Left ventricular geometry and angiogenesis improvement in rat chronic ischemic cardiomyopathy following injection of encapsulated mesenchymal stem cells. *Cell J.* **2022**, *24*, 741–747.

[136] Chen, S. Y.; Zeng, X. D.; Wu, M. F.; Zhu, J. D.; Wu, Y. J. Sodium alginate hydrogel infusion of bone marrow mesenchymal stem cell-derived extracellular vesicles and p38α antagonistic peptides in myocardial infarction fibrosis mitigation. *J. Am. Heart Assoc.* **2025**, *14*, e036887.

[137] Luo, Q. H.; Gao, Z. S.; Liu, J. H.; Wang, Y.; Huang, L. L.; Liu, M. D.; Bai, L.; Gao, Y.; Ye, H. L.; Chen, H. Y. et al. Bioactive peptide-based electroactive hydrogels for myocardial infarction treatment via electrical and microenvironmental regulation. *ACS Appl. Mater. Interfaces* **2025**, *17*, 32066–32080.

[138] Xu, Q. X.; Xiao, Z. Y.; Yang, Q. Z.; Yu, T. T.; Deng, X. J.; Chen, N. H.; Huang, Y. Y.; Wang, L. H.; Guo, J.; Wang, J. H. Hydrogel-based cardiac repair and regeneration function in the treatment of myocardial infarction. *Mater. Today Bio* **2024**, *25*, 100978.

[139] He, S. Y.; Long, L. Y.; Wang, Z. C.; Liu, W. Q.; Zhang, W.; Hu, C.; Wu, X. F.; Dong, R. Q.; Fan, H. S.; Jiang, Q. et al. Combining HUMSC secretome and a conductive hydrogel enhances angiogenesis and electrical transmission at myocardial infarct sites to support cardiac repair. *Chem. Eng. J.* **2023**, *474*, 145877.

[140] Jiao, F.; Qu, Y.; Zhou, G. Q.; Liu, Y.; Li, W.; Ge, C. C.; Li, Y. F.; Hu, W.; Li, B.; Gao, Y. X. et al. Modulation of oxidative stress by functionalized fullerene materials in the lung tissues of female C57/BL mice with a metastatic Lewis lung carcinoma. *J. Nanosci. Nanotechnol.* **2010**, *10*, 8632–8637.

[141] Chen, Y. D.; Xue, Y. G.; Liu, W. H.; Li, S. L.; Wang, X. L.; Zhou, W. X.; Zhang, G. H.; Liu, K.; Zhang, H. J.; Zhao, Y. L. et al. Untethered artificial muscles powered by wearable sweat-based energy generator. *Nano Today* **2023**, *49*, 101765.

[142] Zhang, J.; Shen, S.; Lin, R. R.; Huang, J. X.; Pu, C. Y.; Chen, P. E.; Duan, Q. X.; You, X. T.; Xu, C. Z.; Yan, B. et al. Highly stretchable and biocompatible wrinkled nanoclay-composite hydrogel with enhanced sensing capability for precise detection of myocardial infarction. *Adv. Mater.* **2023**, *35*, 2209497.

[143] Shen, S.; Zhang, J.; Han, Y. N.; Pu, C. Y.; Duan, Q. X.; Huang, J. X.; Yan, B.; You, X. T.; Lin, R. R.; Shen, X. X. et al. A core-shell nanoreinforced ion-conductive implantable hydrogel bioelectronic patch with high sensitivity and bioactivity for real-time synchronous heart monitoring and repairing. *Adv. Healthc. Mater.* **2023**, *12*, 2301990.

[144] Yu, C. J.; Shi, M. Y.; He, S. S.; Yao, M. M.; Sun, H.; Yue, Z. W.; Qiu, Y. W.; Liu, B. J.; Liang, L.; Zhao, Z. M. et al. Chronological adhesive cardiac patch for synchronous mechanophysiological monitoring and electrocoupling therapy. *Nat. Commun.* **2023**, *14*, 6226.

[145] Radisic, M.; Park, H.; Shing, H.; Consi, T.; Schoen, F. J.; Langer, R.; Freed, L. E.; Vunjak-Novakovic, G. Functional assembly of engineered myocardium by electrical stimulation of cardiac myocytes cultured on scaffolds. *Proc. Natl. Acad. Sci. USA* **2004**, *101*, 18129–18134.

[146] Nunes, S. S.; Miklas, J. W.; Liu, J.; Aschar-Sobbi, R.; Xiao, Y.; Zhang, B. Y.; Jiang, J. H.; Massé, S.; Gagliardi, M.; Hsieh, A. et al. Biowire: A platform for maturation of human pluripotent stem cell-derived cardiomyocytes. *Nat. Methods* **2013**, *10*, 781–787.

[147] Hofbauer, P.; Jahnel, S. M.; Papai, N.; Giesshammer, M.; Deyett, A.; Schmidt, C.; Penc, M.; Tavernini, K.; Grdseloff, N.; Meledeth, C. et al. Cardioids reveal self-organizing principles of human cardiogenesis. *Cell* **2021**, *184*, 3299–3317.e22.

[148] Dardano, M.; Kleemiß, F.; Kosanke, M.; Lang, D.; Wilson, L.; Franke, A.; Teske, J.; Shivaraj, A.; de la Roche, J.; Fischer, M. et al. Blood-generating heart-forming organoids recapitulate co-development of the human haematopoietic system and the embryonic heart. *Nat. Cell Biol.* **2024**, *26*, 1984–1996.

[149] Park, B.; Park, J.; Han, S. H.; Kwon, T.; Sung, J. Y.; Kim, J.; Safarkhani, M.; Min, K. H.; Lee, E. H.; Kang, S. M. et al. Advances in organoid-on-a-chip for recapitulation of human physiological events. *Mater. Today* **2025**, *84*, 75–94.

[150] Mak, I. W.; Evaniew, N.; Ghert, M. Lost in translation: Animal models and clinical trials in cancer treatment. *Am. J. Transl. Res.* **2014**, *6*, 114–118.

[151] Zhou, W. X.; Zhang, K.; Chen, H.; Rahman, M. S. U.; Wang, L. X.; Li, S. L.; Wang, C. H.; Liu, Y.; Xu, S. S. Stable and efficient animal models of the peritoneal adhesion. *Adv. Ther.* **2023**, *6*, 2300093.

[152] Xia, X. J.; Hu, M. E.; Zhou, W. Y.; Jin, Y. P.; Yao, X. D. Engineering cardiology with miniature hearts. *Mater. Today Bio* **2025**, *31*, 101505.

[153] Cho, S.; Discher, D. E.; Leong, K. W.; Vunjak-Novakovic, G.; Wu, J. C. Challenges and opportunities for the next generation of cardiovascular tissue engineering. *Nat. Methods* **2022**, *19*, 1064–1071.

[154] Ryu, H.; Wang, X. L.; Xie, Z. Q.; Kim, J.; Liu, Y. G.; Bai, W. B.; Song, Z.; Song, J. W.; Zhao, Z. C.; Kim, J. et al. Materials and design approaches for a fully bioresorbable, electrically conductive and mechanically compliant cardiac patch technology. *Adv. Sci.* **2023**, *10*, 2303429.

[155] Williams, D. F. On the mechanisms of biocompatibility. *Biomaterials* **2008**, *29*, 2941–2953.

[156] Crawford, L.; Wyatt, M.; Bryers, J.; Ratner, B. Biocompatibility evolves: Phenomenology to toxicology to regeneration. *Adv. Healthc. Mater.* **2021**, *10*, 2002153.

[157] Hu, C.; Liu, W. Q.; Wang, J.; Hua, C.; Long, L. Y.; Yang, X.; Lu, L.; Zhu, Y.; Yang, L.; Wang, Y. B. et al. Injectable hydrogels with

tailored recombinant humanized collagen type I for the repair of damaged hearts by remodeling the myocardial microenvironment. *Collagen Leather* **2025**, *7*, 38.

[158] Xu, Z.; Li, X. J.; Mi, X. L.; Lin, Y. Y. Exosomes loaded stimuli responsive conductive hydrogel restores cardiac function post-myocardial infarction via SIRT1/p53-mediated anti-inflammatory mechanism: Mechanistic insights into cardioprotection. *Biomater. Adv.* **2026**, *180*, 214610.

[159] Yang, Z. Y.; Zhang, Y. J.; Wang, J. N.; Yin, J. B.; Wang, Z.; Pei, R. J. Cardiac organoid: Multiple construction approaches and potential applications. *J. Mater. Chem. B* **2023**, *11*, 7567–7581.

[160] Drakhlis, L.; Biswanath, S.; Farr, C. M.; Lupanow, V.; Teske, J.; Ritzenhoff, K.; Franke, A.; Manstein, F.; Bolesani, E.; Kempf, H. et al. Human heart-forming organoids recapitulate early heart and foregut development. *Nat. Biotechnol.* **2021**, *39*, 737–746.

[161] Fan, C. X.; He, J. X.; Xu, S. J.; Yan, J. Y.; Jin, L. F.; Dai, J. W.; Hu, B. W. Advances in biomaterial-based cardiac organoids. *Biomater. Adv.* **2023**, *153*, 213502.

[162] Li, J. Y.; Yao, Y. J.; Zhou, J. Y.; Yang, Z. H.; Qiu, C.; Lu, Y. W.; Xie, J. Q.; Liu, J.; Jiang, T. Y.; Kou, Y. H. et al. Epicardial transplantation of antioxidant polyurethane scaffold based human amniotic epithelial stem cell patch for myocardial infarction treatment. *Nat. Commun.* **2024**, *15*, 9105.

[163] Varzideh, F.; Mone, P.; Santulli, G. Bioengineering strategies to create 3D cardiac constructs from human induced pluripotent stem cells. *Bioengineering* **2022**, *9*, 168.

[164] Silva, A. C.; Matthys, O. B.; Joy, D. A.; Kauss, M. A.; Natarajan, V.; Lai, M. H.; Turaga, D.; Blair, A. P.; Alexanian, M.; Bruneau, B. G. et al. Co-emergence of cardiac and gut tissues promotes cardiomyocyte maturation within human iPSC-derived organoids. *Cell Stem Cell* **2021**, *28*, 2137–2152.e6.

[165] Liu, C.; Feng, X.; Li, G. P.; Gokulnath, P.; Xiao, J. J. Generating 3D human cardiac constructs from pluripotent stem cells. *EBioMedicine* **2022**, *76*, 103813.

[166] Song, M.; Choi, D. B.; Im, J. S.; Song, Y. N.; Kim, J. H.; Lee, H.; An, J.; Kim, A.; Choi, H.; Kim, J. C. et al. Modeling acute myocardial infarction and cardiac fibrosis using human induced pluripotent stem cell-derived multi-cellular heart organoids. *Cell Death Dis.* **2024**, *15*, 308.

[167] Wang, F. F.; Xu, Z. L.; Zheng, F. Y.; Yang, D. C.; Xu, K. G.; Ke, M.; Zhou, X.; Zhang, X. H.; Tan, J.; Liu, Y. et al. Cardiac organoid model inspired micro-robot smart patch to treat myocardial infarction. *Adv. Mater.* **2025**, *37*, 2417327.

[168] Tan, Y.; Coyle, R. C.; Barrs, R. W.; Silver, S. E.; Li, M.; Richards, D. J.; Lin, Y. L.; Jiang, Y. W.; Wang, H. J.; Menick, D. R. et al. Nanowired human cardiac organoid transplantation enables highly efficient and effective recovery of infarcted hearts. *Sci. Adv.* **2023**, *9*, eadf2898.

[169] Gu, B. S.; Han, K.; Cao, H. B.; Huang, X. X.; Li, X.; Mao, M.; Zhu, H.; Cai, H.; Li, D. C.; He, J. K. Heart-on-a-chip systems with tissue-specific functionalities for physiological, pathological, and pharmacological studies. *Mater. Today Bio* **2024**, *24*, 100914.

[170] Xu, F.; Jin, H.; Liu, L. L.; Yang, Y. Y.; Cen, J. Z.; Wu, Y. B.; Chen, S. Y.; Sun, D. H. Architecture design and advanced manufacturing of heart-on-a-chip: Scaffolds, stimulation and sensors. *Microsyst. Nanoeng.* **2024**, *10*, 96.

[171] Liu, B. Q.; Wang, S. Y.; Ma, H.; Deng, Y. L.; Du, J. C.; Zhao, Y. M.; Chen, Y. Heart-on-a-chip: A revolutionary organ-on-chip platform for cardiovascular disease modeling. *J. Transl. Med.* **2025**, *23*, 132.

[172] Campbell, S. B.; Wu, Q. H.; Yazbeck, J.; Liu, C.; Okhovatian, S.; Radisic, M. Beyond polydimethylsiloxane: Alternative materials for fabrication of organ-on-a-chip devices and microphysiological systems. *ACS Biomater. Sci. Eng.* **2021**, *7*, 2880–2899.

[173] Liu, S. T.; Wang, Z. H.; Chen, X. Y.; Han, M. Y.; Xu, J.; Li, T.; Yu, L.; Qin, M. Y.; Long, M.; Li, M. C. et al. Multiscale anisotropic scaffold integrating 3D printing and electrospinning techniques as a heart-on-a-chip platform for evaluating drug-induced cardiotoxicity. *Adv. Healthc. Mater.* **2023**, *12*, 2300719.

[174] Hu, L. L.; Han, M. Y.; Yang, J. X.; Yu, L.; Qin, M. Y.; Xu, J.; Zhang, H.; Chen, X. Y.; Li, Y. M.; Meng, H. F. et al. Engineering cardiobundles with dynamic microenvironmental control as advanced cardiac modeling for heart-on-a-chip. *Small* **2025**, *21*, 2505617.

[175] Rexius-Hall, M. L.; Khalil, N. N.; Escopete, S. S.; Li, X.; Hu, J. Y.; Yuan, H. Y.; Parker, S. J.; McCain, M. L. A myocardial infarct border-zone-on-a-chip demonstrates distinct regulation of cardiac tissue function by an oxygen gradient. *Sci. Adv.* **2022**, *8*, eabn7097.

[176] Veldhuizen, J.; Chavan, R.; Moghadas, B.; Park, J. G.; Kodibagkar, V. D.; Migrino, R. Q.; Nikkhah, M. Cardiac ischemia on-a-chip to investigate cellular and molecular response of myocardial tissue under hypoxia. *Biomaterials* **2022**, *281*, 121336.

[177] Kim, J.; Zhang, X. N.; Wang, R.; Najer, A.; Lau, Q. Y.; Cammack-Najera, A.; Kim, J. A.; Kang, Y. K.; Xie, R. X.; Kim, H. et al. Vascularized and perfusable human heart-on-a-chip model recapitulates aspects of myocardial ischemia and enables analysis of nanomedicine delivery. *Adv. Mater.* **2025**, *37*, e18909.

[178] Gao, Z.; Du, Z. Y.; Hou, Y.; Hua, K.; Tu, P. F.; Ai, X. N.; Jiang, Y. A microfluidic coculture model for mapping signaling perturbations and precise drug screening against macrophage-mediated dynamic myocardial injury. *Acta Pharm Sin. B* **2024**, *14*, 5393–5406.

[179] Sun, L. Y.; Chen, Z. Y.; Xu, D. Y.; Zhao, Y. J. Electroconductive and anisotropic structural color hydrogels for visual heart-on-a-chip construction. *Adv. Sci.* **2022**, *9*, 2105777.

[180] Esmaeili, H.; Zhang, Y. N.; Ravi, K.; Neff, K.; Zhu, W. Q.; Migrino, R. Q.; Park, J. G.; Nikkhah, M. Development of an electroconductive heart-on-a-chip model to investigate cellular and molecular response of human cardiac tissue to gold nanomaterials. *Biomaterials* **2025**, *320*, 123275.

[181] Han, J. L.; Xu, X. Y.; Li, J. H.; Zhang, H. Y.; Su, W. G.; Wang, K.; Li, H. M.; Xu, Z. P.; Chen, J.; Cai, X. X. et al. Mechanically matched heart-on-a-chip platform mediated maturation of excitation-contraction coupling. *ACS Nano* **2025**, *19*, 24052–24066.

[182] Wang, W.; Su, W. G.; Han, J. L.; Song, W.; Li, X. Y.; Xu, C. H.; Sun, Y.; Wang, L. Microfluidic platforms for monitoring cardiomyocyte electromechanical activity. *Microsyst. Nanoeng.* **2025**, *11*, 4.

[183] Li, J. X.; Gu, B. S.; Chang, J. K.; Zhang, B.; Yao, C.; Ma, Q. H.; Han, K.; Li, D. C.; He, J. K. One-step laser-assisted electrohydrodynamic printing of microelectronic scaffolds for electrophysiological monitoring of aligned cardiomyocytes. *ACS Nano* **2025**, *19*, 15775–15788.

[184] Zhang, K.; Wang, P.; Wu, L. L.; Wang, S. R.; Jia, Y. L.; Yang, J. A soft patch for dynamic myocardial infarction monitoring. *ACS Appl. Mater. Interfaces* **2025**, *17*, 16479–16488.

[185] Juguilon, C.; Khosravi, R.; Radisic, M.; Wu, J. C. *In vitro* modeling of interorgan crosstalk: Multi-organ-on-a-chip for studying cardiovascular-kidney-metabolic syndrome. *Circ. Res.* **2025**, *136*, 1476–1493.

[186] Gao, E. H.; Lei, Y. H.; Shang, X. Y.; Huang, Z. M.; Zuo, L.; Boucher, M.; Fan, Q.; Chuprun, J. K.; Ma, X. L.; Koch, W. J. A novel and efficient model of coronary artery ligation and myocardial infarction in the mouse. *Circ. Res.* **2010**, *107*, 1445–1453.

[187] Zhang, L. H.; Bei, Z. W.; Li, T.; Qian, Z. Y. An injectable conductive hydrogel with dual responsive release of rosmarinic acid improves cardiac function and promotes repair after myocardial infarction. *Bioact. Mater.* **2023**, *29*, 132–150.

[188] Liu, Z. B.; Yang, P. C.; Tian, Y. M.; Deng, H. Y.; Xia, J. J.; Li, B. H.; Wu, B. Y.; Fang, Y. C.; Xiong, Z.; Zhang, T. A microneedle substrate-based sutureless engineered cardiac patch for myocardial infarction repair. *Bio-Des. Manuf.* **2025**, *8*, 917–929.

[189] Zhu, S. J.; Yu, C. J.; Liu, N. B.; Zhao, M. Y.; Chen, Z. R.; Liu, J.; Li, G.; Huang, H. L.; Guo, H. M.; Sun, T. C. et al. Injectable conductive

gelatin methacrylate / oxidized dextran hydrogel encapsulating umbilical cord mesenchymal stem cells for myocardial infarction treatment. *Bioact. Mater.* **2022**, *13*, 119–134.
[190] Salameh, A.; Dhein, S. Effects of mechanical forces and stretch on intercellular gap junction coupling. *Biochim. Biophys. Acta Biomembr.* **2013**, *1828*, 147–156.
[191] Zhang, X.; Wang, X. L.; Xu, M. M.; Yuan, J.; Liu, Y. Monocyte/macrophage-mediated trained immunity in disease prevention and immunotherapy. *Bioact. Mater.* **2026**, *59*, 745–762.
[192] Tang, J. L.; Chen, Z. Y.; Sun, B. Y.; Dong, J. Q.; Liu, J.; Zhou, H. G.; Wang, L. M.; Bai, R.; Miao, Q.; Zhao, Y. L. et al. Polyhydroxylated fullerenols regulate macrophage for cancer adoptive immunotherapy and greatly inhibit the tumor metastasis. *Nanomed: Nanotechnol. Biol. Med.* **2016**, *12*, 945–954.
[193] Chen, P. E.; Zhang, W.; Fan, X. L.; Shi, X.; Jiang, Y. N.; Yan, L. W.; Li, H. K.; Wang, C. M.; Han, L.; Lu, X. et al. A polyphenol-derived redox-active and conductive nanoparticle-reinforced hydrogel with wet adhesiveness for myocardial infarction repair by simultaneously stimulating anti-inflammation and calcium homeostasis pathways. *Nano Today* **2024**, *55*, 102157.
[194] Cheng, N. L.; Luo, Q.; Yang, Y. Q.; Shao, N.; Nie, T. Q.; Deng, X. J.; Chen, J. F.; Zhang, S. Q.; Huang, Y. Y.; Hu, K. et al. Injectable pH responsive conductive hydrogel for intelligent delivery of metformin and exosomes to enhance cardiac repair after myocardial ischemia-reperfusion injury. *Adv. Sci.* **2025**, *12*, 2410590.
[195] Zhang, Y.; Zhu, D. S.; Wei, Y. Z.; Wu, Y. F.; Cui, W. L.; Liuqin, L.; Fan, G. W.; Yang, Q.; Wang, Z. X.; Xu, Z. L. et al. A collagen hydrogel loaded with HDAC7-derived peptide promotes the regeneration of infarcted myocardium with functional improvement in a rodent model. *Acta Biomater.* **2019**, *86*, 223–234.
[196] Huang, K.; Zhu, D. S.; Soto, J.; Hu, S. Q.; Fang, J.; Huang, J.; Zhang, X. X.; Li, J. L.; Li, Y.; Tasoudis, P. et al. Immunomodulatory microneedle patch for cardiac repair in rodent and porcine models of myocardial infarction. *Cell Biomater.* **2025**, *1*, 100152.
[197] Zuo, X. H.; Xiao, Y.; Yang, J.; He, Y. M.; He, Y. X.; Liu, K.; Chen, X. P.; Guo, J. L. Engineering collagen-based biomaterials for cardiovascular medicine. *Collagen Leather* **2024**, *6*, 33.
[198] Paul, A.; Hasan, A.; Kindi, H. A.; Gaharwar, A. K.; Rao, V. T. S.; Nikkhah, M.; Shin, S. R.; Krafft, D.; Dokmeci, M. R.; Shum-Tim, D. et al. Injectable graphene oxide/hydrogel-based angiogenic gene delivery system for vasculogenesis and cardiac repair. *ACS Nano* **2014**, *8*, 8050–8062.
[199] Xu, K.; Liu, Y.; Chen, C. Y. Future prospects in clinical translation of inorganic nanoparticles. *Acta Pharm Sin. B* **2024**, *14*, 5082–5084.
[200] Wang, H. X.; Li, L.; Luo, L. H.; Cheng, Y. Q.; Zhou, F.; Zhao, S. J.; Li, Y.; Yang, Y. Z.; Zhou, Q. Q.; Niu, H. Y. et al. Advanced nanomaterial platforms for targeted therapy of myocardial ischemia-reperfusion injury. *Research* **2025**, *8*, 0822.
[201] Wang, Z. X.; Qin, C.; Liao, Z. B.; Zhang, H. J.; Lu, H. X.; Xiao, Y.; Wu, C. T. Inorganic biomaterials inducing scaffolds pre-neuralization for infarcted myocardium repair. *Adv. Mater.* **2025**, *37*, 2419765.
[202] Kim, C.; Kim, H.; Sim, W. S.; Jung, M.; Hong, J.; Moon, S.; Park, J. H.; Kim, J. J.; Kang, M.; Kwon, S. et al. Spatiotemporal control of neutrophil fate to tune inflammation and repair for myocardial infarction therapy. *Nat. Commun.* **2024**, *15*, 8481.
[203] Liu, W. Q.; Long, L. Y.; Wang, Z. C.; He, S. Y.; Han, Y. L.; Yang, L.; Hu, C.; Wang, Y. B. A Whole-course-repair system based on stimulus-responsive multifunctional hydrogels for myocardial tissue regeneration. *Small Methods* **2024**, *8*, 2400121.
[204] Lin, C. B.; Huang, X.; Xue, Y. G.; Jiang, S. S.; Chen, C. Y.; Liu, Y.; Chen, K. Advances in medical devices using nanomaterials and nanotechnology: Innovation and regulatory science. *Bioact. Mater.* **2025**, *48*, 353–369.